A Stepwise Electron-Transfer Relay Mimicking the Primary Charge Separation in Bacterial Photosynthetic Reaction Center

Atsuhiro Osuka,[*,1a] **Shinji Marumo,**[1a] **Noboru Mataga,**[*,1b] **Seiji Taniguchi,**[1c] **Tadashi Okada,**[*,1c] **Iwao Yamazaki,**[1d] **Yoshinobu Nishimura,**[1d] **Takeshi Ohno,**[1e] **and Koichi Nozaki**[1e]

Contribution from the Department of Chemistry, Faculty of Science, Kyoto University, Kyoto 606, Japan, Institute for Laser Technology, Utsubo-Honmachi 1-8-4, Osaka 550, Japan, Department of Chemistry, Faculty of Engineering Science and Research Center for Extreme Materials, Osaka University, Toyonaka 560, Japan, Department of Chemical Process Engineering, Faculty of Engineering, Hokkaido University, Sapporo 060, Japan, and Department of Chemistry, Faculty of Science, Osaka University, Toyonaka 560, Japan

Received June 26, 1995[⊗]

Abstract: The synthesis and excited-state dynamics are described for zinc-methylenechlorin−porphyrin−pyromellitimide triads, ZC−HP−I and ZC−ZP−I, and related dyads ZC−HP, ZC−ZP, HP−I, and ZP−I, where ZC, HP, ZP, and I indicate a zinc-methylenechlorin, a free-base porphyrin, a zinc-porphyrin, and pyromellitimide, respectively. In the steady-state fluorescence spectra of ZC−HP, ZC−HP−I, ZC−ZP, and ZC−ZP−I, only the emission from ZC is commonly observed, indicating efficient intramolecular singlet−singlet excitation energy transfer from HP or ZP to ZC. ZC−HP−I undergoes a stepwise electron-transfer relay: ^{1}(ZC)*−HP−1 → (ZC)$^+$−(HP)$^-$−I → (ZC)$^+$−HP−(I)$^-$ with overall quantum yields of 0.70 and 0.07 in THF and DMF, respectively. In ZC−ZP−I, a pre-formed equilibrium between ^{1}(ZC)*−ZP−I and (ZC)$^+$−(ZP)$^-$−I is followed by a rapid charge-shift reaction to provide a secondary ion-pair state (ZC)$^+$−ZP−(I)$^-$ with the overall quantum yield of 0.90 and 0.47 in THF and DMF, respectively. The intermediate ion-pair state (ZC)$^+$−(ZP)$^-$−I is stabilized enough so as to be clearly detected in DMF, while it is slightly higher in energy than ^{1}(ZC)* in THF, rendering its detection difficult.

Introduction

In relation to the photoinduced charge separation mechanism in natural photosynthetic reaction centers (RC), many model compounds have been prepared in order to better understand factors which control electron-transfer reactions in these highly complex systems.[2−6] The determination of the three-dimensional structures of the bacterial RC[7] has exerted a great impact on such investigations. Recently, much attention has been focused on conformationally restricted, structurally and energetically well-defined models, since they have provided useful data for analysis of factors which control electron-transfer rates and have been demonstrated to mimic some aspects of photosynthetic energy and electron transfers.[4−6,8−14,19−21] Nevertheless, the achievement of a RC-like sequential electron-transfer relay or superexchange electron transfer in artificial molecular systems still remains very difficult with respect to the efficiency of charge separation as well as the reaction mode. The advantage

of multistep electron transfer strategy has been amply demonstrated with many models during the past decade.[4−6] To date, however, most of them belong to a class of donor(D)−pigment-(P)−acceptor(A) type triads in which charge separation between a pigment and an electron acceptor gives D−(P)$^+$−(A)$^-$ as an initial ion pair which undergoes a subsequent hole transfer,

[⊗] Abstract published in *Advance ACS Abstracts,* December 15, 1995.

(1) (a) Kyoto University. (b) Institute for Laser Technology. (c) Faculty of Engineering Science, Osaka University. (d) Hokkaido University. (e) Faculty of Science, Osaka University.

(2) Boxer, S. G. *Biochim. Biophys. Acta* **1983**, *726*, 265.

(3) Connolly, J. S.; Bolton, J. R. In *Photoinduced Electron Transfer, Part D*; Fox, M. A., Chanon, M., Eds.; Elsevier: Amsterdam, 1988; p 303.
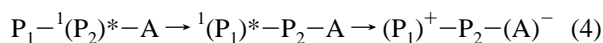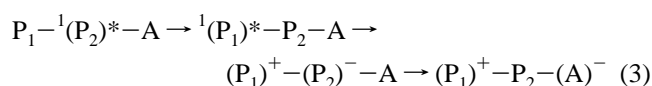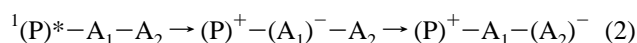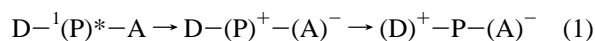
(4) (a) Wasielewski, M. R. *Photochem. Photobiol.* **1988**, *47*, 923. (b) Wasielewski, M. R. In *Photoinduced Electron Transfer, Part A*; Fox, M. A., Chanon, M., Eds.; Elsevier: Amsterdam, 1988; p 161. (c) Wasielewski, M. R. *Chem. Rev.* **1992**, *92*, 435.

(5) Gust, D.; Moore, T. A. *Science* **1989**, *244*, 35. Gust, D.; Moore, T. A.; Moore, A. L. *Acc. Chem. Res.* **1993**, *26*, 198.

(6) Maruyama, K.; Osuka, A. *Pure Appl. Chem.* **1990**, *62*, 1511. Maruyama, K.; Osuka, A.; Mataga, N. *Pure Appl. Chem.* **1994**, *66*, 867.

(7) (a) Deisenhofer, J.; Epp, O.; Miki, K.; Huber, R.; Michel, H. *J. Biol. Chem.* **1984**, *180*, 385. (b) Chang, C.-H.; Tiede, D. M.; Tang, J.; Norris, J. R.; Schiffer, M. *FEBS Lett.* **1986**, *205*, 82. (c) Allen, J. P.; Feher, G.; Yeates, T. O.; Komiya, H.; Rees, D. C. *Proc. Natl. Acad. Sci. U.S.A.* **1987**, *84*, 5730.

(8) (a) Brun, A. M.; Harriman, A.; Heitz, V.; Savauge, J. P. *J. Am. Chem. Soc.* **1991**, *113*, 8657. (b) Heiler, D.; McLendon, G.; Rogalskyj, P. *J. Am. Chem. Soc.* **1987**, *109*, 604. (c) Sessler, J. L.; Capuano, V. L.; Harriman, A. *J. Am. Chem. Soc.* **1993**, *115*, 4618. (d) Zaleski, J.; Wu, W.; Chang, C. K.; Leroi, G. E.; Cukier, R. I.; Nocera, D. G. *Chem. Phys.* **1993**, *176*, 483. (e) Pöllinger, Heitele, H.; Michel-Beyerle, M. E.; Anders, C.; Futscher, M.; Staab, H. A. *Chem. Phys. Lett.* **1992**, *198*, 645. (f) Lawson, J. M.; Paddon-Row, M. N. *J. Chem. Soc., Chem. Commun.* **1993**, 1641.

(9) (a) Wasielewski, M. R.; Niemczyk, M. P.; Svec, W. A.; Pewitt, E. B. *J. Am. Chem. Soc.* **1985**, *107*, 5562. (b) Wasielewski, M. R.; Gaines III, G. L.; O'Neil, M. P.; Svec, W. A., Niemczyk, M. P. *J. Am. Chem. Soc.* **1990**, *112*, 4559.

(10) (a) Osuka, A.; Nagata, T.; Kobayashi, F.; Zhang, R. P.; Maruyama, K.; Mataga, N.; Asahi, T.; Ohno, T.; Nozaki, K. *Chem. Phys. Lett.* **1992**, *199*, 302. (b) Osuka, A.; Yamada, H.; Maruyama, K.; Ohno, T.; Nozaki, K.; Okada, T.; Tanaka, Y.; Mataga, N. *Chem. Lett.* **1995**, 591. (c) Osuka, A.; Zhang, R. P.; Maruyama, K.; Ohno, T.; Nozaki, K. *Chem. Lett.* **1993**, 1727. (d) Osuka, A.; Zhang, R. P.; Maruyama, K.; Ohno, T.; Nozaki, K. *Bull. Chem. Soc. Jpn.* **1993**, *66*, 3773. (e) Osuka, A.; Zhang, R. P.; Maruyama, K.; Mataga, N.; Tanaka, Y.; Okada, T. *Chem. Phys. Lett.* **1993**, *215*, 179.

(11) (a) Osuka, A.; Nakajima, S.; Maruyama, K.; Mataga, N.; Asahi, T. *Chem. Lett.* **1991**, 1003. (b) Osuka, A.; Nakajima, S.; Maruyama, K.; Mataga, N.; Asahi, T.; Yamazaki, I.; Nishimura, Y.; Ohno, T.; Nozaki, K. *J. Am. Chem. Soc.* **1993**, *115*, 4577.

(12) (a) Nishitani, S.; Kurata, N.; Sakata, Y.; Misumi, S.; Karen, A.; Okada, T.; Mataga, N. *J. Am. Chem. Soc.* **1983**, *105*, 7771. (b) Mataga, N.; Karen, A.; Okada, T.; Nishitani, S.; Kurata, N.; Sakata, Y.; Misumi, S. *J. Phys. Chem.* **1984**, *88*, 5138.

(13) Gust, D.; Moore, T. A.; Moore, A. L.; Macpherson, A. N.; Lopez, A.; DeGraziano, J. M.; Gouni, I.; Bittersman, E.; Seely, G. R.; Nieman, R. A.; Ma, X. C.; Demanche, L. J.; Hung, S. C.; Luttrull, D. K.; Lee, S. J.; Kerrigan, P. K. *J. Am. Chem. Soc.* **1993**, *115*, 11141.

(14) Ohkohchi, M.; Takahashi, A.; Mataga, N.; Okada, T.; Osuka, A.; Yamada, H.; Maruyama, K. *J. Am. Chem. Soc.* **1993**, *115*, 12137.

providing $(D)^+ - P - (A)^-$ as a secondary ion-pair (eq 1).[5,6,9−11] In another strategy, $P - A_1 - A_2$ triads have been developed, where a charge-shift reaction in the initial ion pair $(P)^+ - (A_1)^- - A_2$ provides a long-lived charge separated state $(P)^+ - A_1 - (A_2)^-$ (eq 2).[12−14] However, the reaction sequences of eqs 1 and 2 differ from the natural electron-transfer relay in the RC, in that the initial electron transfer is not a charge separation between tetrapyrrole pigments.[15] In view of more closer mimicry, we are interested in making a triad of $P_1 - P_2 - A$, in which the following reaction sequence can be realized within a single molecule; (1) the light energy captured by pigments P_1 and P_2 is once collected at P_1, then (2) the first electron transfer starts from $^1(P_1)^*$ to P_2 to give $(P_1)^+ - (P_2)^- - A$ and a subsequent charge-shift reaction affords $(P_1)^+ - P_2 - (A)^-$ (eq 3), or (3) a one-step, long-distance electron transfer (superexchange) from $^1(P_2)^*$ to A gives $(P_1)^+ - P_2 - (A)^-$ directly (eq 4), and (4) the secondary ion pair $(P_1)^+ - P_2 - (A)^-$ thus formed is fairly long-lived. In addition, it is obviously favorable that quantum yield for formation of $(P_1)^+ - P_2 - (A)^-$ would be made quite high. Whether the monomeric bacteriochlorophyll is a real, intermediate electron carrier or serves as a superexchange mediator is still one of the most controversial issues concerning the primary photochemistry in bacterial photosynthesis. Therefore, synthetic triads that follow the reaction sequence of eqs 3 and/or 4 are very interesting in relation to the issue of superexchange vs sequential mechanism.[16−18]

$$D - {}^1(P)^* - A \rightarrow D - (P)^+ - (A)^- \rightarrow (D)^+ - P - (A)^- \quad (1)$$

$${}^1(P)^* - A_1 - A_2 \rightarrow (P)^+ - (A_1)^- - A_2 \rightarrow (P)^+ - A_1 - (A_2)^- \quad (2)$$

$$P_1 - {}^1(P_2)^* - A \rightarrow {}^1(P_1)^* - P_2 - A \rightarrow$$
$$(P_1)^+ - (P_2)^- - A \rightarrow (P_1)^+ - P_2 - (A)^- \quad (3)$$

$$P_1 - {}^1(P_2)^* - A \rightarrow {}^1(P_1)^* - P_2 - A \rightarrow (P_1)^+ - P_2 - (A)^- \quad (4)$$

Recently, several groups have observed that nonradiative decay of a distal $^1(P_1)^*$ in covalently-linked $P_1 - P_2 - A$ triads can be enhanced by the electronic interaction with the attached acceptor A even in cases where through-space electronic interaction between $^1(P_1)^*$ and A is negligibly small.[19−21] For example, in conformationally restricted triads consisting of free-

base porphyrin (H_2P), zinc-porphyrin (ZnP), and quinone (Q), Sessler et al. have reported remarkably effective long-distance electron transfer from the distal H_2P to Q.[19] They have interpreted such electron transfer in terms of a direct zinc-porphyrin-mediated superexchange mechanism. We have also reported similar long-distance electron transfer from the distal H_2P to the acceptor in related models such as $H_2P - ZnP - Q$ and $H_2P - ZnP - $pyromellitimide (I).[21] In these cases, unfortunately however, the ion-pair state could not be detected by transient absorption spectroscopy. In only a few successful cases, Wasielewski et al. have reported pyropheophorbide−porphyrin−electron acceptor triads, which provide a (pyropheophorbide)$^+$−porphyrin−(electron acceptor)$^-$ ion-pair state in high yields by a direct, long-distance electron transfer.[20b,c] On the basis of the dependence of the long-distance electron transfer rate on the nature and energy of the intervening porphyrin chromophore, they proposed that mixing of the π-orbitals of the porphyrin and chlorophyll leads to a state with charge transfer character which relaxes to the final IP state. They have further explored another set of triads where a keto functionality in the zinc-pyropheophorbide is reduced to a secondary alcohol in order to enhance its electron donating ability.[20b] These models undergo a single step, long-distance, photoinduced ET within several picoseconds even at 77 K in 2-methyltetrahydrofuran.

Here we provide the synthesis and excited-state dynamics of a new set of zinc methylenechlorin−porphyrin−pyromellitimide triads ZC−HP−I and ZC−ZP−I, where ZC, ZP, HP, and I indicate a zinc-methylenechlorin and a β-unsubstituted zinc-porphyrin, a β-unsubstituted free-base porphyrin, and a pyromellitimide acceptor, respectively (Chart 1). We chose a ZC subunit because of its low S_1-energy as well as its low one-electron oxidation potential. ZC/HP and ZC/ZP combinations have favorable energetic relationships for desired intramolecular charge separations. Pyromellitimide electron acceptor is quite useful for analysis of electron transfer kinetics because of the characteristic absorption spectrum of its anion radical[11] and a pertinent one-electron reduction potential for our purpose. In addition, anion radicals of HP and ZP both exhibit distinct absorption bands in the near-infrared region, greatly facilitating analysis of electron-transfer dynamics. In the triads, the two macrocycles are held at a fixed distance (the center-to-center distance between ZC and P is ca. 12.8 Å) with an extended coplanar orientation and the center-to-center distance between P and I is fixed to be ca. 13 Å. We have also prepared ZC−HP and ZC−ZP dyads, HP−I and ZP−I dyads, and parent chromophores ZC, HP, and ZP in order to understand the various events which follow from excitation of the triads.

Results

Synthesis of Models. Synthesis of ZC−HP−I and ZC−ZP−I is shown in Schemes 1 and 2. Porphyrin **4** was prepared by the cross condensation reaction of aldehydes **1** and **3** with 3,3′,4,4′-tetraethyldipyrrylmethane **2**[22] under our standard condi-

(15) Two examples have appeared, where the initial charge separation between tetrapyrrole pigments triggers the formation of fully charge separated ion-pair states, a carotenoid (C)−zinc porphyrin (ZP)−free-base porphyrin (HP) triad [(a) Gust, D.; Moore, T. A.; Moore, A. L.; Leggett, L.; Lin, S.; DeGraziano, J. M.; Hermant, R. M.; Nicodem, D.; Craig, P.; Seely, G. R.; Nieman, R. A. *J. Phys. Chem*. **1993**, *97*, 7926] and a zinc porphyrin (ZP)−oxochlorin (HC)−pyromellitimide (I) triad [(b) Osuka, A.; Marumo, S.; Maruyama, K.; Mataga, N.; Tanaka, Y.; Taniguchi, S.; Okada, T.; Yamazaki, I.; Nishimura, Y. *Bull. Chem. Soc. Jpn*. **1995**, *68*, 262]. Proposed reaction routes for the secondary ion pairs are as following; $C - ZP - {}^1(HP)^* \rightarrow C - (ZP)^+ - (HP)^- \rightarrow (C)^+ - ZP - (HP)^-$ in the former and $ZP - {}^1(HC)^* - I \rightarrow (ZP)^+ - (HC)^- - I \rightarrow (ZP)^+ - (HC) - (I)^-$ in the latter model.

(16) (a) Martin, J.-L.; Breton, J.; Hoff, A. J.; Migus, A.; Antonetti, A. *Proc. Natl. Acad. Sci. U.S.A*. **1986**, *83*, 957. (b) Kirmaier, C.; Holten, D. *Proc. Natl. Acad. Sci. U.S.A*. **1990**, *87*, 3552.

(17) (a) Holtzapfel, W.; Finkele, U.; Kaiser, W.; Oesterhelt, D.; Scheer, H.; Stilz, H. U.; Zinth, W. *Chem. Phys. Lett*. **1989**, *160*, 1. (b) Arlt, T.; Schmidt, S.; Kaiser, W.; Lauterwasser, C.; Meyer, M.; Scheer, H.; Zinth, W. *Proc. Natl. Acad. Sci. U.S.A*. **1993**, *90*, 11757.

(18) Bixon, M.; Jortner, J.; Michel-Beyerle, M. E. *Biochim. Biophys. Acta* **1991**, *1056*, 301. (b) Chan, C.-K.; Chen, L. X.; DiMagno, T. J.; Hanson, D. K.; Nance, S. L.; Schiffer, M.; Norris, J. R.; Flemming, G. R. *Chem. Phys. Lett*. **1991**, *176*, 366. (c) Du, M.; Rosenthal, S. J.; Xie, X.; DiMagno, T. J.; Schmidt, M.; Hanson, D. K.; Schiffer, M.; Norris, J. R.; Flemming, G. R. *Proc. Natl. Acad. Sci. U.S.A*. **1992**, *89*, 8517.

(19) Sessler, J. S.; Johnson, M. R.; Lin, T. Y.; Creager, S. E. *J. Am. Chem. Soc*. **1988**, *110*, 3659. Sessler, J. S.; Johnson, M. R.; Lin, T. Y. *Tetrahedron* **1989**, *45*, 4767. Rodriguez, J.; Kirmaier, C.; Johnson, M. R.; Friesner, R. A.; Holten, D.; Sessler, J. L. *J. Am. Chem. Soc*. **1991**, *113*, 1652.

(20) (a) Wasielewski, M. R.; Johnson, D. G.; Niemczyk, M. P.; Gaines, III, G. L.; O'Neil, M. P.; Svec, W. A. *J. Am. Chem. Soc*. **1990**, *112*, 6482. (b) Johnson, D. G.; Niemczyk, m. P.; Minsek, D. W.; Wierrerrechy, G. P.; Svec, W. A.; Gaines, III, G. L.; Wasielewski, M. R. *J. Am. Chem. Soc*. **1993**, *115*, 5692. (c) Wiederrecht, G. P.; Watanabe, S.; Wasielewski, M. R. *Chem. Phys*. **1993**, *176*, 601. (d) Wasielweski, M. R.; Gaines, G. L. III, Wiederrecht, G. P.; Svec, W. A.; Niemczyk, M. P. *J. Am. Chem. Soc*. **1993**, *115*, 10442.

(21) (a) Osuka, A.; Maruyama, K.; Mataga, N.; Asahi, T.; Yamazaki, I.: Tamai, N.; Nishimura, Y. *Chem. Phys. Lett*. **1991**, *181*, 413. (b) Osuka, A.; Nagata, T.; Maruyama, K.; Mataga, N.; Asahi, T.; Yamazaki, I.; Nishimura, Y. *Chem. Phys. Lett*. **1991**, *185*, 88. (c) Nagata, T. *Bull. Chem. Soc. Jpn*. **1991**, *64*, 3005. (d) Osuka, A.; Marumo, S.; Taniguchi, S. Okada, T.; Mataga, N. *Chem. Phys. Lett*. **1994**, *230*, 144.

(22) Ono, N.; Kawamura, H.; Bougauchi, M.; Maruyama, K. *Tetrahedron* **1990**, *46*, 7483.

Scheme 1. Synthesis of Oxochlorin **6**[a]
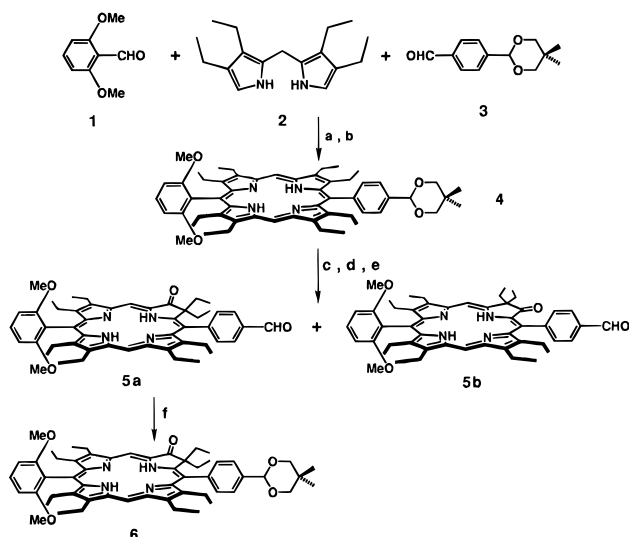
[a] (a) CCl$_3$CO$_2$H/MeCN, 12 h; (b) *p*-chloranil, THF, 4 h; (c) OsO$_4$, pyridine/CH$_2$Cl$_2$, 24 h; (d) H$_2$S, 1 h; (e) TFA, 10% H$_2$SO$_4$, CHCl$_3$, reflux, 12 h; and (f) 2,2-dimethyl-1,3-propanediol, *p*-TsOH, benzene, reflux, 10 h.

tions.[23] The dimethoxy substituents at the meso-aryl group were introduced in order to increase steric hindrance for OsO$_4$ oxidation at the near pyrrole, thereby inducing regioselective oxidation at the opposite pyrrole.[15b] In fact, the oxidation of **4** followed by treatment with H$_2$S and hydrolysis with trifluoroacetic acid gave oxochlorins **5a** and **5b**.[15b,24] Oxidation products at the near pyrrole were scarcely detected. Formyl group in the major product **5a** was protected as an acetal to give **6** which was transformed into hydroxychlorin **7** by the procedure developed by Chang (MeLi/ether).[25] We found that dehydration of **7** was carried out more cleanly upon heating with trifluoroacetic acid in the presence of neopentyl alcohol, giving methylenechlorin **8** in 84% yield. The acetal protection group in **8** was hydrolyzed to give **9** which was finally condensed with dipyrrylmethane **10**[26] and pyromellitimide-linked aldehyde **11**[27] to furnish methylenechlorin−porphyrin−pyromellitimide **12** (HC−HP−I) in 51% yield based on the amount of **9** used.[28] Careful metalation of **12** with Zn(OAc)$_2$ yielded ZC−ZP−I and ZC−HP−I in 46 and 13% yields, respectively. Dyads ZC−HP and ZC−ZP were prepared in essentially the same manner. ZC, HP−I, ZP−I, HP, and ZP were also prepared as reference molecules. All these models were fully characterized by 500 MHz ^{1}H NMR and FAB mass spectra. The ^{1}H-NMR spectra of these models are nearly solvent independent, being consistent with expected constrained geometries of these models.

Absorption and Fluorescence Spectra. The ground-state absorption spectra of ZC−HP−I, ZC−ZP−I, HP−I, and ZP−I are almost solvent-independent and identical to the corresponding pyromellitimide-free compounds ZC−HP, ZC−ZP, HP, and ZP, respectively, indicating that attachment of the pyromellitimide moiety to the macrocycles with a -phenyl-CH$_2$- spacer does not significantly perturb their electronic structure. The absorption spectra of ZC−HP−I and ZC−ZP−I in THF are
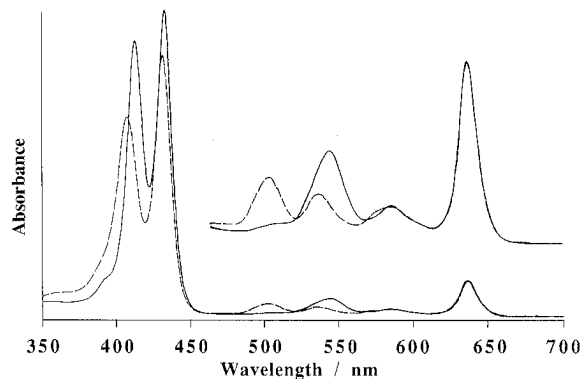
(23) Nagata, T.; Osuka, A.; Maruyama, K. *J. Am. Chem. Soc.* **1990**, *112*, 3054.

(24) (a) Chang, C. K.; Sotiriou, C. *J. Org. Chem.* **1985**, *50*, 4989. (b) Osuka, A.; Maruma, S.; Maruyama, K. *Bull. Chem. Soc. Jpn.* **1993**, *66*, 3837.

(25) Chang, C. K. *Biochemistry* **1980**, *19*, 1971.

(26) Chong, R.; Clezy, P. S.; Liepa, A. J.; Nichol, A. W. *Aust. J. Chem.* **1969**, *22*, 229.

(27) Nagata, T. *Bull. Chem. Soc. Jpn.* **1991**, *64*, 3005.

(28) Manka, J. S.; Lawrence, D. S. *Tetrahedron Lett.* **1989**, *33*, 6989. DiMango, S. G.; Lin, V. S.-Y.; Therien, M. J. *J. Org. Chem.* **1993**, *58*, 5983.

Figure 1. UV−visible absorption spectra of ZC−HP−I (− −) and ZC−ZP−I (−) in THF.

shown in Figure 1. The ground-state absorption spectra can be adequately described as a superposition of the respective spectra of ZC and HP or ZP. Distinct B-bands are observed at 407 (HP) and 431 (ZC) nm and at 412 (ZP) and 430 (ZC) nm in the spectra of ZC−HP−I and ZC−ZP−I, respectively. The B-bands of HP and ZP are blue-shifted by ca. 1 nm and the B-bands of ZC are red-shifted by 3−4 nm, respectively, relative to the position of the reference monomer. This fact suggests that there are weak electronic interactions between the two macrocycles. On the other hand, the absorption spectra in the Q-band region are described as the simple sum of the respective chromophores. Qy-bands of ZC in ZC−ZP−I and ZC−HP−I are observed at 636 and 637 nm, respectively, being virtually the same as that (636 nm) of reference ZC. In the steady-state fluorescence spectra of ZC−HP−I, ZC−HP, ZC−ZP−I, and ZC−ZP, only the emission from ZC is commonly observed (Figures 2 and 5). The emission bands of ZC in ZC−ZP−I and ZC−HP−I are both observed at 638 nm, being ca. 2 nm blue-shifted from that of reference ZC. Later we will discuss the fluorescence spectra and the transient absorption spectra of these molecules taken for excitation at 637 or 635 nm, where the molecular extinction coefficients are ca. 5 × 10^4 and ca. 1500 M^{-1} cm^{-1} for ZC and HP, respectively, and ZP has no absorbance.

Estimation of Energy Levels. Table 1 summarizes the energy levels of the locally excited singlet states of the chromophore and the hypothetical ion-pair states. The energies of the excited states are determined by averaging the energies of the corresponding (0,0) peaks in the fluorescence and absorption bands in each solvent. First the energies of ion-pair states in DMF are estimated from the simple sum of the one-electron oxidation and reduction potentials; the one-electron oxidation potentials of ZC, ZP, and HP are −0.06, 0.43, and 0.61 V vs ferrocene/ferrocenium ion, and the one-electron reduction potentials of HP, ZP, and I are −1.61, −1.87, and −1.24 V, respectively. Later, we will refine these estimates using a correction term which has been obtained from analysis of biphasic fluorescence decay due to thermal repopulation of the singlet excited state from ion-pair state according to the procedure reported earlier.[29] The energies in benzene and THF are estimated with corrected solvation energies calculated by the Born equation,[30] and those in THF will be again corrected in the same way as in DMF.

Energetically important features are the following: (1) an energy gradient exists for ZC−HP−I in the order of ^{1}(HP)* ≥ ^{1}(ZC)* > (ZC)$^+$−(HP)$^-$ > (ZC)$^+$−HP−(I)$^-$ in both THF and

(29) (a) Gaines, G. L.; O'Neil, M. P.; Svec, W. A.; Niemczyk, M. P.; Wasielewski, M. R. *J. Am. Chem. Soc.* **1991**, *113*, 719. (b) Asahi, T.; Ohkohchi, M.; Matsusaka, R.; Mataga, N.; Zhang, R.-P.; Osuka, A.; Maruyama, K. *J. Am. Chem. Soc.* **1993**, *115*, 5665.

(30) Weller, A. *Z. Phys. Chem. (Wiesbaden)* **1982**, *93*, 1982.

Scheme 2. Synthesis of ZC−HP−I and ZC−ZP−I Triads[a]
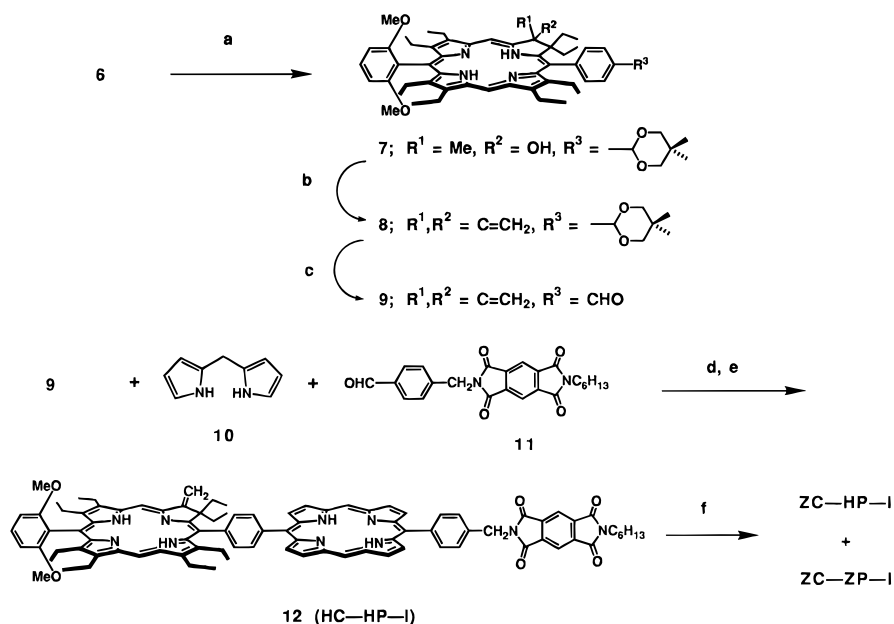
[a] (a) methyl lithium/ether, 1.5 h; (b) TFA, 2,2-dimethyl-1,3-propanediol, benzene, reflux, 6 h; (c) TFA, 10% H_2SO_4, $CHCl_3$, reflux, 6 h; (d) TFA/CH_2Cl_2, 24 h; (e) DDQ, 12 h; and (f) Zn(OAc)$_2$, 30 min.

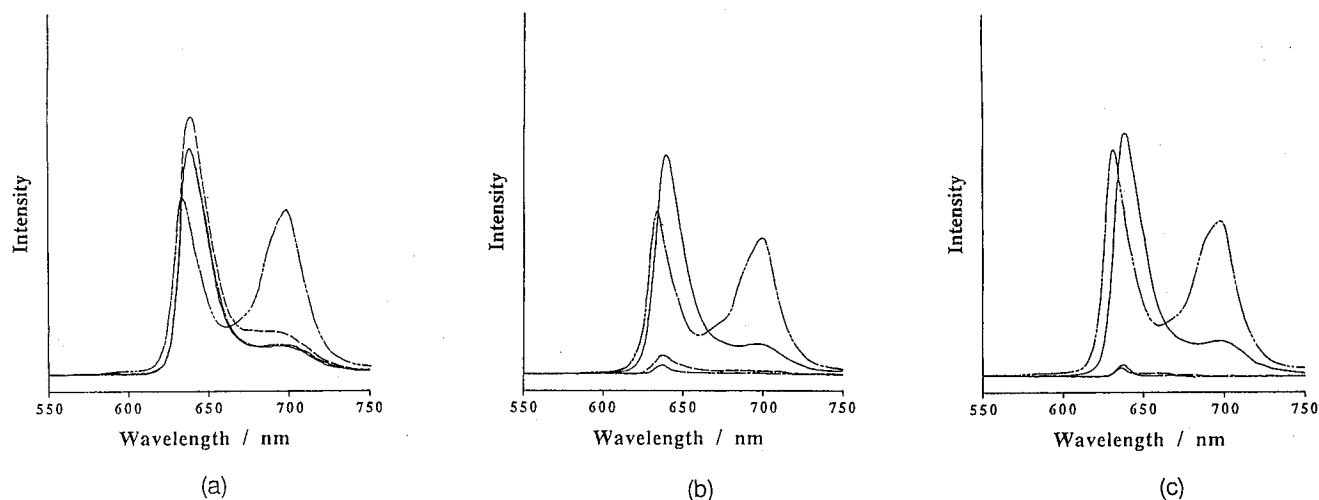**Figure 2.** Steady-state fluorescence spectra of ZC (−), ZC−HP (− −), ZC−HP−I (− · −), and HP (− ·· −) taken for excitation at 637 nm (a) in benzene, (b) in THF, and (c) in DMF. The absorbances at 637 nm were adjusted to be 0.1.

DMF, which may allow a "stepwise" electron-transfer relay of ^{1}(ZC)*−HP−I → (ZC)$^+$−(HP)$^-$−I → (ZC)$^+$−HP−(I)$^-$, and (2) for ZC−ZP−I, the similar gradient, ^{1}(ZP)* > ^{1}(ZC)* > (ZC)$^+$−(ZP)$^-$ > (ZC)$^+$−ZP−(I)$^-$, is found in DMF, while ^{1}(ZC)* is nearly isoenergetic to (ZC)$^+$−(ZP)$^-$ in less polar THF.

Photoexcited-State Dynamics. In order to understand sometimes complicated photochemistry of the triads, it is appropriate to consider first some simpler compounds which constitute parts of the triads.

HP−I, ZC−HP, and ZC−HP−I. Comparison of the fluorescence quantum yields of HP−I and HP has revealed no fluorescence quenching in ^{1}(HP)*−I in THF and DMF. This has been also confirmed by the measurements of fluorescence lifetimes and picosecond transient absorption spectra; the fluorescence lifetime is the same as that of the reference HP, and there is no trace of the characteristic absorption due to (I)$^-$ in the transient absorption spectra. In DMF, the energy level of (HP)$^+$−(I)$^-$ is lower in energy than ^{1}(HP)*−I (Table 1), but the charge separation does not occur. Probably, the driving force seems to be insufficient to overcome the requisite large reorganization.

Models ZC−HP and ZC−HP−I exhibit fluorescence only from ^{1}(ZC)* even for preferential excitation at HP. This fact indicates the efficient intramolecular singlet−singlet energy transfer from HP to ZC. This is supported by the fluorescence excitation spectra of ZC−HP and ZC−HP−I that are almost identical with the absorption spectra. Figure 2 shows the fluorescence spectra of ZC−HP and ZC−HP−I in benzene, THF, and DMF, along with those of ZC and HP taken for selective excitation at the ZC moiety. In benzene, the fluorescence intensity from ^{1}(ZC)*−HP is nearly the same as that of ZC (Figure 2a), while the intensity is sharply reduced in THF and DMF (Figure 2b,c). The fluorescence decay curves of ^{1}-(ZC)*−HP and ^{1}(ZC)*−HP−I can be reproduced by a singlet exponential function with short lifetimes of 12−16 ps in THF and DMF (Table 2); the fluorescence lifetimes of ^{1}(ZC)*−HP and ^{1}(ZC)*−HP−I are nearly the same.

The transient absorption of ZC−HP spectra taken in THF (Figure 3a) and in DMF (Figure 4a) have revealed that this efficient fluorescence quenching is due to an intramolecular charge separation. In THF, characteristic transient absorption bands at 450 and 870 nm that are both due to (HP)$^-$ grow up
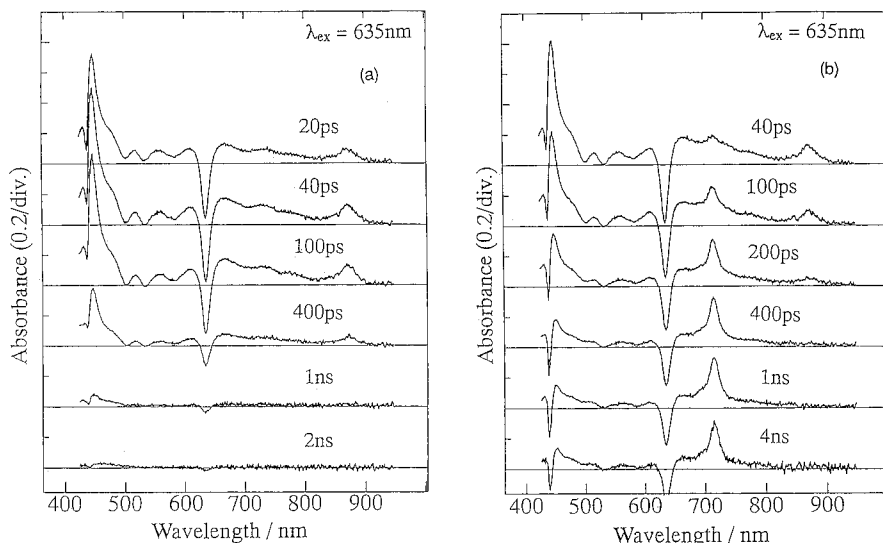
Figure 3. Time-resolved transient absorption spectra of ZC—HP (a) and ZC—HP—I (b) in THF taken for excitation at 635 nm.

Table 1. Estimated Energy Levels for the S_1-States and Charge Separated States[a,b]

model	benzene	THF	DMF
^{1}ZC*	1.94	1.94	1.94
^{1}HP*	1.96	1.96	1.96
^{1}ZP*	2.13	2.13	2.13
(HP)$^+$—(I)$^-$	2.74	2.06 (2.09)	1.85 (1.93)
(ZP)$^+$—(I)$^-$	2.56	1.88 (1.91)	1.67 (1.75)
(ZC)$^+$—(ZP)$^-$	2.39	1.94 (1.97)	1.81 (1.89)
(ZC)$^+$—(HP)$^-$	2.13	1.68 (1.71)	1.55 (1.63)
(ZC)$^+$—P—(I)$^-$	2.29	1.46 (1.49)	1.18 (1.26)

[a] The energy levels of the excited states were determined on the basis of the corresponding fluorescence and absorption (0,0) bands. The energy of the ion pair states in DMF were a simple sum of the electrochemical potential of the respective chromophore; the one-electron oxidation potentials of HP, ZP, and ZC are 0.61, 0.43, and -0.06 V vs ferrocene/ferrocenium ion, and the one-electron reduction potentials of HP, ZP, and I are -1.61, -1.87, and -1.24 V. The energy levels of the ion pair states in benzene and THF were estimated by: $E(\text{IP}) = E_{ox} - E_{red} + \Delta G_s$, $\Delta G_s = (e^2/2)(1/r_D + 1/r_A)(1/4\pi\epsilon_0\epsilon - 1/4\pi\epsilon_0\epsilon_r) - e^2/4\pi\epsilon_0\epsilon R_{DA}$, where E_{ox} and E_{red} are oxidation and reduction potentials of donor and acceptor, respectively measured in DMF, r_D and r_A are effective radii of donor cation and acceptor anion, and ϵ_r and ϵ are dielectric constants of DMF and benzene or THF, respectively. The radii of (ZC)$^+$, (P)$^+$, and (P)$^-$ were estimated to be 5.5 Å, and the radius of (I)$^-$ was estimated to be 3.5 Å, and the separation (R_{DA}) between charges was estimated to be 12.8 Å for (ZC)$^+$—(P)$^-$, 13.0 Å for (P)$^+$—(I)$^-$, and 24.4 Å for (ZC)$^+$—P—(I)$^-$, respectively. [b] Numbers in the parentheses indicate the corrected energy levels, see text.

with a time constant of 20 ps and then decay with a time constant of 400 ps. Bleaching of the ZC Qy-band at 636 nm is observed immediately upon laser excitation and is found to recover with the same 400-ps time constant. These spectral changes clearly indicate a rapid formation of (ZC)$^+$—(HP)$^-$ and its decay to the ground state. By simulating the time-profile of the 450- and 870-nm bands, rates of charge separation (k_{CS1}) and charge recombination (k_{CR1}) have been determined to be 4.9×10^{10} and 2.5×10^9 s^{-1}, respectively. Similar analysis of the transient spectra in Figure 4a has provided the intramolecular electron transfer rate constants: $k_{CS1} = 9.9 \times 10^{10}$ and $k_{CR1} = 3.3 \times 10^{10}$ s^{-1} in DMF. These rates of the charge separation are in good agreement with the rates, 4.9 and 7.5×10^{10} s^{-1} in THF and DMF, respectively, obtained using the fluorescence lifetimes by the following equations: $k_{CS1} = 1/\tau(\text{ZCH}) - 1/\tau_0$-(ZC), where $\tau(\text{ZCH})$ is the fluorescence lifetime of ^{1}(ZC)*—HP and $\tau_0(\text{ZC})$ is the fluorescence lifetime of the reference ZC (Table 2). It is worthy to note that the charge recombination in (ZC)$^+$—(HP)$^-$ is considerably accelerated in polar DMF solution, as have been frequently observed in intramolecular

Scheme 3. Reaction Scheme of ZC—HP—I
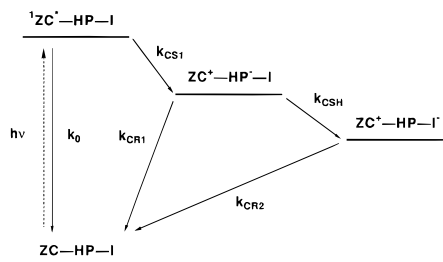
charge-recombination reaction of distance-fixed donor—acceptor systems lying in the Marcus inverted region.[11,29b,31]

Now it is of great interest whether an electron in the HP moiety in (ZC)$^+$—(HP)$^-$—I can move to the pyromellitimide acceptor in competition with energy-wasteful charge recombination to the ground state. This has been examined by the transient absorption spectroscopy on ZC—HP—I.

In THF (Figure 3b), the 450- and 870-nm transient absorptions due to (HP)$^-$ appear initially with a time constant of 20 ps and decay with a time constant of 120 ps. The rise time constant is the same as that of ZC—HP, but the decay time constant is considerably shorter in comparison to ZC—HP. Decay of the transient absorption bands of (HP)$^-$ is accompanied by a rise of the 716-nm absorption band of (I)$^-$ with a time constant of 120 ps, clearly indicating the occurrence of a charge-shift reaction, (ZC)$^+$—(HP)$^-$—I → (ZC)$^+$—HP—(I)$^-$. On the basis of these findings, the reaction scheme of ZC—HP—I in THF can be written as shown in Scheme 3. Rate constant of charge-shift reaction (k_{CSH}) has been determined to be 5.8×10^9 s^{-1} by the following equation; $k_{CSH} = 1/\tau(\text{ion 2}) - 1/\tau(\text{ion 1})$, where $\tau(\text{ion 1})$ and $\tau(\text{ion 2})$ are the lifetimes of (ZC)$^+$—(HP)$^-$ and (ZC)$^+$—(HP)$^-$—I, respectively. According to Scheme 3, the quantum yield for formation of the secondary ion pair can be calculated by $\Phi = k_{CS1}/(k_0 + k_{CS1}) \times k_{CSH}/(k_{CSH} + k_{CR1})$ to be 0.69 in THF. Charge-recombination kinetics of (ZC)$^+$—HP—(I)$^-$ to the ground state have been found to follow a biphasic decay with time constants of 110 (42%) and 400 ns (58%). Biphasic decay behavior is rather common for the related P$_1$—P$_2$—A triads bearing a 1,4-phenylene spacer between

(31) (a) Closs, G. L.; Miller, J. R. *Science* **1988**, *240*, 440. (b) Antolovich, M.; Keyte, P. J.; Oliver, A. M.; Paddon-Row, M. N.; Kroon, J.; Verhoeven, J. W.; Jonker, A. A.; Warman, J. M. *J. Phys. Chem.* **1991**, *95*, 1933. (c) Irvine, M. P.; Harrison, R. J.; Beddard, G. S.; Leighton, P.; Sanders, J. K. M. *Chem. Phys.* **1986**, *104*, 315.
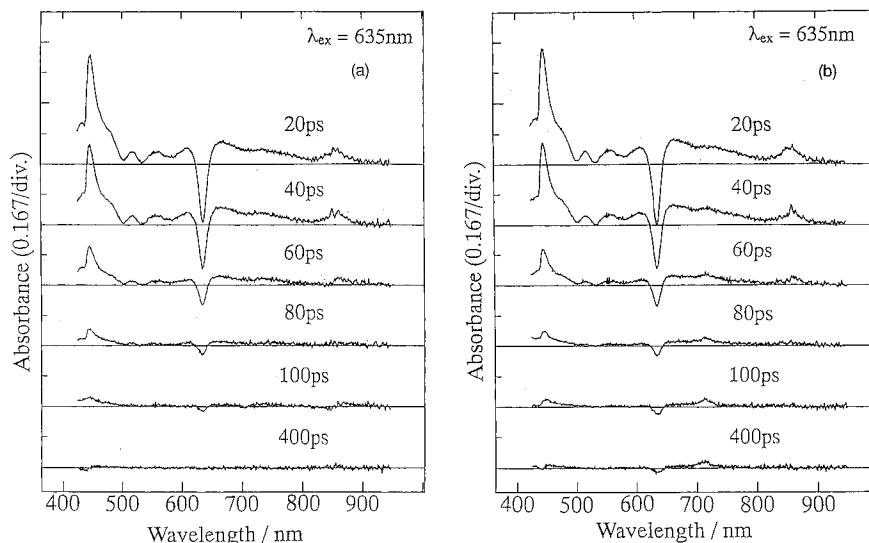
Figure 4. Time-resolved transient absorption spectra of ZC−HP (a) and ZC−HP−I (b) in DMF taken for excitation at 635 nm.

Table 2. Fluorescence Lifetimes (ps) of ZC Moieties[a,b]

	ZC	ZC−HP−I	ZC−HP	ZC−ZP−I	ZC−ZP
benzene	680	740	920	680	700
THF	790	15	16	39(0.22), 217(0.78)	38(0.33), 880(0.67)
DMF	860	12	13	32(0.62), 72(0.38)	41(0.50), 89(0.50)

[a] Fluorescence decays were measured at 640 nm for excitation at 625 nm. Except decay curves of ZC−ZP−I and ZC−ZP in THF and DMF, the other decaying curves were satisfactorily fitted with single exponential functions. [b] Numbers in parentheses are relative amplitudes of pre-exponential factors in double exponential functions.

P_1 and P_2.[10] Careful studies on the external magnetic field effects on this decay revealed that singlet−triplet intersystem crossing in the singlet radical ion pair competes with the charge recombination to the ground state.[32] This causes the biphasic decay of the ion pair to the ground state.

In DMF, essentially the same type of a step-wise electron-transfer has been revealed by the transient absorption spectra (Figure 4b). However, the amount of the secondary ion pair $(ZC)^+-HP-(I)^-$ is quite small. In essentially the same manner, k_{CSH} value and Φ have been estimated to be 2.4×10^9 s^{-1} and 0.07, respectively. As will be described in more detail later, the overall quantum yield for the formation of the secondary ion pair can be determined on the basis of the absorbances of the initial excited state and the secondary ion-pair state. Following this method, the quantum yield has been determined to be 0.70 and 0.07 in THF and DMF, respectively,[33] in good agreement with the estimation based on the kinetic data. The low value of Φ is due mostly to very efficient charge recombination in the initial $(ZC)^+-(HP)^--I$ ion pair in polar DMF, since the k_{CSH} values are quite similar in THF and DMF. These results indicate the importance of the solvent polarity in determining the overall quantum yield. Although the effect of polar environment on k_{CS1} and k_{CSH} is rather small, it increases k_{CR}. These phenomena must be common for distance-fixed

(32) Udo, W.; Sakaguchi, Y.; Hayashi, H.; Nohya, G.; Yoneshima, R.; Nakajima, S.; Osuka, A. *J. Phys. Chem.* **1995**, *99*, 13930. In these triad ion pairs, the rates of the charge separation to the ground state (10^6-10^7 s^{-1}) are comparable to the rates of the singlet−triplet intersystem crossing. Therefore, the ion pairs decay either directly to the ground state (faster component) or via the triplet ion-pair followed by the reverse intersystem crossing and the charge recombination in the singlet ion-pair (slower component). Applied magnetic field suppressed the intersystem crossing, thereby enhancing the biphasicity. The absence of a second component in DMF is now under study.

(33) The difference absorption coefficients used are $\epsilon((ZC)^+-(HP)^-)_{450}$ $= 1.1 \times 10^5$, $\epsilon((ZC)^+-(HP)^-)_{715} = 2.0 \times 10^4$, $\epsilon((ZC)^+-(HP)^-)_{872} = 2.2$ $\times 10^4$ M^{-1} cm^{-1} in THF, and $\epsilon((ZC)^+-(HP)^-)_{450} = 1.1 \times 10^5$, $\epsilon((ZC)^+-(HP)^-)_{715} = 2.0 \times 10^4$, $\epsilon((ZC)^+-(HP)^-)_{860} = 2.2 \times 10^4$ M^{-1} cm^{-1} in DMF. The other absorption coefficients are the same as those used for the analysis of the excited-state dynamics of ZC−ZP−I.

triads P_1-P_2-A and should be taken into consideration in future molecular design.

ZP−I, ZC−ZP, and ZC−ZP−I. ZP is a better electron donor and a poor electron acceptor than HP. In fact, we observed the fluorescence quenching in ZP−I in THF and DMF. The fluorescence lifetimes are shortened to 630 ps in THF and 570 ps in DMF in comparison to those of ZP reference: 2.49 ns in THF and 2.55 ns in DMF. By the transient absorption spectroscopy (not shown), the intramolecular charge separation giving $(ZP)^+-(I)^-$ has been revealed to be a major additional nonradiative decaying route of $^1(ZP)^*-I$. In THF the 716-nm absorption due to $(ZP)^+-(I)^-$ shows a rise with 70 ps time constant and a decay with 630 ps time constant that is exactly the same with the fluorescence lifetime of $^1(ZP)^*-I$. Based on these data, rates of the charge separation (k_{CS2}) and charge recombination (k_{CR2}) have been determined to be 1.2×10^9 and 1.4×10^{10} s^{-1}. In DMF, we could not detect the ion-pair state clearly, presumably owing to the rapid charge recombination. Estimated rates in DMF are $k_{CS2} = 1.4 \times 10^9$ and $k_{CR2} \gg 1 \times 10^{10}$ s^{-1} in DMF. In both solvents, the values of k_{CR2} are much larger than the values of k_{CS2}. The rate constants of charge separation (k_{CS2}) in $^1(ZP)^*-I$ can also be estimated with the fluorescence lifetimes using the following equation: $k_{CS2} = 1/\tau(ZPI) - 1/\tau_0(ZP)$, where $\tau(ZPI)$ is the fluorescence lifetime of ZP−I and $\tau_0(ZP)$ is the fluorescence lifetime of the reference ZP. Rate constants thus estimated are 1.2×10^9 and 1.4×10^9 s^{-1} in THF and DMF, respectively, in good agreement with the results based on the transient spectra.

The fact that only the emission from $^1(ZC)^*$ is observed indicates the occurrence of efficient energy transfers, ZC−^{1}(ZP)* → ^{1}(ZC)*−ZP and ZC−^{1}(ZP)*−I → ^{1}(ZC)*−ZP−I. The fluorescence excitation spectrum of ZC−ZP is identical with its absorption spectrum, again indicating that such energy transfer is nearly quantitative. Short-lived fluorescence emission from ZC−^{1}(ZP)* can be observed by the picosecond time-resolved fluorescence measurement, and its lifetime has been determined to be 15 ps in THF and 24 ps in DMF. Based on
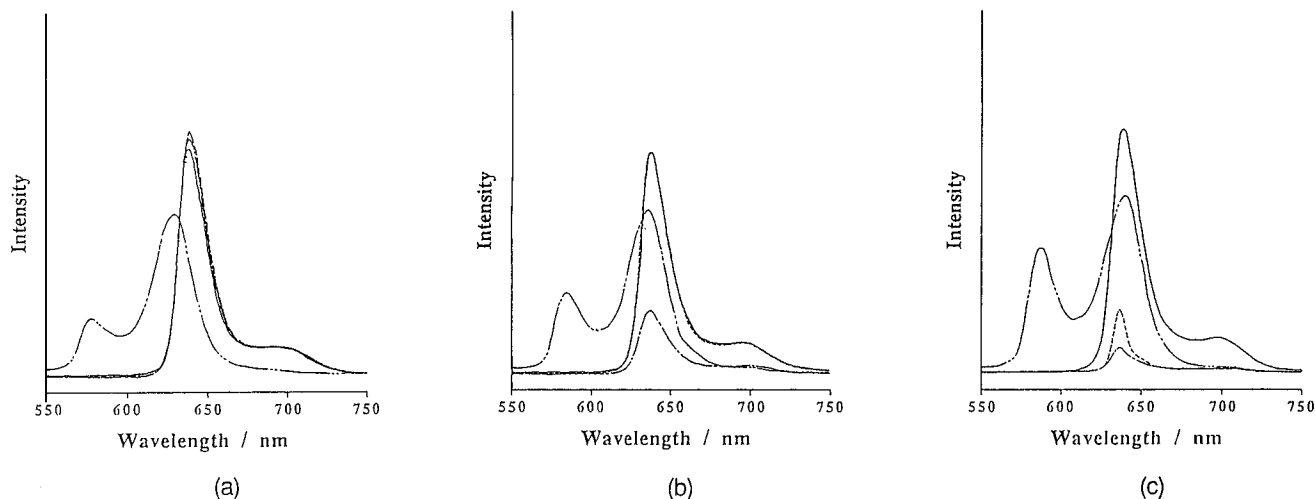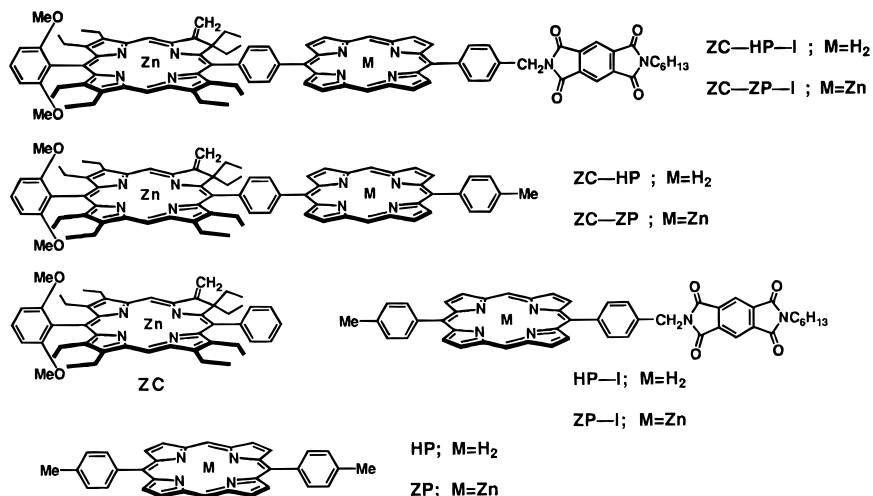
Stepwise Electron-Transfer Relay

J. Am. Chem. Soc., Vol. 118, No. 1, 1996 161

Figure 5. Steady-state fluorescence spectra of ZC (−), ZC−ZP (− −), and ZC−ZP−I (− · −) taken for excitation of 637 nm, (a) in benzene, (b) in THF, and (c) in DMF. The absorbances at 637 nm were adjusted to be 0.1. Fluorescence spectrum of Zp (− ·· −) was also shown for comparison.

Chart 1. Structures of the models Studied in This Paper

these results the rate constants of the excitation energy transfer (k_{EN}) have been determined using the following equation: $k_{EN} = 1/\tau(ZP) - 1/\tau_0(ZP)$, where $\tau(ZP)$ is the fluorescence lifetime of the ZC−^{1}(ZP)*, to be 6.6×10^{10} and 4.1×10^{10} s^{-1} in THF and DMF, respectively. Since these k_{EN} rates are ca. 30−50 times larger than k_{CS2} in ^{1}(ZP)*−I subunit, we can conclude that the energy transfer from ZC−^{1}(ZP)*−I to ^{1}(ZC)*−ZP−I is much preferential over an electron transfer to give ZC−(ZP)$^+$−(I)$^-$. In addition, we can selectively excite the ZC moiety at 635−637 nm. This excitation is very helpful and allows us to examine their excited-state dynamics starting from ^{1}(ZC)*. The steady-state fluorescence spectra taken for such excitation (Figure 5) are again solvent polarity dependent, indicating the solvent-polarity dependent excited-state dynamics. We will discuss the excited-state dynamics first in polar DMF and then in less polar THF on the basis of the transient spectra obtained by excitation at 635 nm.

In DMF, the fluorescence quantum yields of ZC−ZP and ZC−ZP−I relative to that of the reference ZC are 0.26 and 0.10, respectively (Figure 5c). As will be discussed later, this fluorescence quenching has been shown, by the transient absorption spectra, due to the the intramolecular charge separation to give (ZC)$^+$−(ZP)$^-$ and (ZC)$^+$−(ZP)$^-$−I. It was not possible to reproduce the fluorescence decay curve of ^{1}(ZC)*−ZP by a single-exponential formula, but a double exponential formula gave a good fit with $\tau_1 = 89$ ps (50%) and $\tau_2 = 41$ ps (50%) ($\chi^2 = 0.99$), indicating an intrinsic biphasic decay of the ^{1}(ZC)*−ZP. Most probably this behavior is due to the thermal

repopulation of ^{1}(ZC)*−ZP from (ZC)$^+$−(ZP)$^-$ ion pair.[29,34] Scheme 4a illustrates a kinetic model which accounts for the data. From this scheme, the decay function of the relative fluorescence intensity is given by eqs 5−8

$$I_f(t) = C_1 \exp(\mu_1 t) + C_2 \exp(-\mu_2 t) \qquad (5)$$

$$\mu_{1,2} = (1/2)[-\tau_0^{-1} + k_{CS1} + k_{ret} + k_{CR1} \mp \{(k_{ret} + k_{CR1} - \tau_0^{-1} - k_{CS1})^2 + 4k_{CS1}k_{ret}\}^{1/2}] \qquad (6)$$

$$C_1 = (\tau_0^{-1} + k_{CS1} - \mu_2)/(\mu_1 - \mu_2) \qquad (7)$$

$$C_2 = (\tau_0^{-1} + k_{CS1} - \mu_1)/(\mu_1 - \mu_2) \qquad (8)$$

where C_1 and C_2 are the relative amplitude of pre-exponential factors, and μ_1 and μ_2 are the reciprocal of the respective fluorescence lifetimes. The observed biphasic decay curve has been analyzed by eqs 5−8, giving following values of rate constants: $k_{CS1} = 1.7 \times 10^{10}$, $k_{CR1} = 1.5 \times 10^{10}$, and $k_{ret} = 2.7 \times 10^9$ s^{-1}. The transient absorption spectra of ZC−ZP in DMF (Figure 6a) indicates the formation of (ZC)$^+$−(ZP)$^-$ and its decay to the ground state; the 450- and 883-nm transient absorptions are both due to (ZP)$^-$. Based on this kinetic scheme, the time-profiles at 450 and 883 nm were adequately reproduced by using the respective difference absorption coefficients; ϵ(^{1}-

(34) Heitele, H.; Finck, S.; Weeren, S.; Pollinger, F.; Michel-Beyerle, M. *J. Phys. Chem.* **1989**, *93*, 5173.
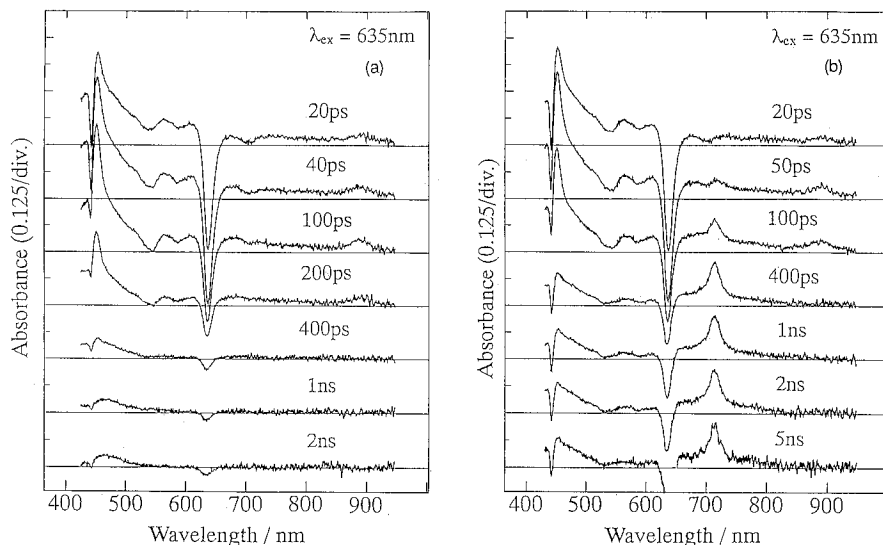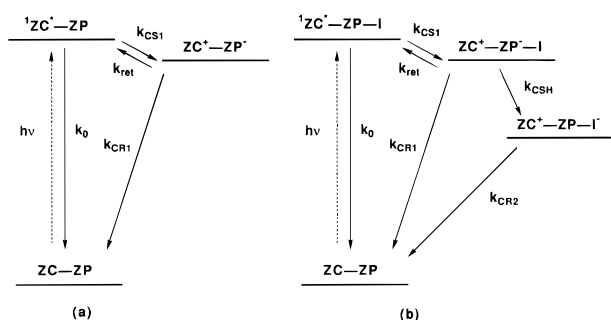
Figure 6. Time-resolved transient absorption spectra of ZC−ZP (a) and ZC−ZP−I (b) in DMF taken for excitation at 635 nm.

Scheme 4. Reaction Schemes of ZC−ZP (a) and ZC−ZP−I (b) in DMF

$(ZC)*)_{450} = 3.8 \times 10^4$, $\epsilon(^1(ZC)*)_{883} = 4.0 \times 10^3$, $\epsilon((ZC)^+-(ZP)^-)_{450} = 1.38 \times 10^5$, $\epsilon((ZC)^+-(ZP)^-)_{883} = 1.6 \times 10^4$, $\epsilon(^3(ZC)*)_{450} = 5.0 \times 10^4$, and $\epsilon(^3(ZC)*)_{883} = 2.0 \times 10^3$ M^{-1} cm^{-1} (Figure 7). Through this fitting procedure we have obtained the values of $k_{CS1} = 1.4 \times 10^{10}$, $k_{CR1} = 1.1 \times 10^{10}$, and $k_{ret} = 2.4 \times 10^9$ s^{-1}, in good agreement with the analysis based on the fluorescence lifetime. The energy difference ΔG between $^1(ZC)*$ and $(ZC)^+-(ZP)^-$ can be determined directly from the relationship $\Delta G = -RT \ln (k_{CS1}/k_{ret})$. This provides the energy of the ion-pair state 0.05 eV below that of $^1(ZC)*$. This estimation is ca. 0.08 eV higher than the energy estimated on the basis of the electrochemical data. We use this difference as a correction term for the estimation of the ion-pair energy,[29] and the corrected energies are also listed in Table 1.

As is the case for ZC−ZP, ZC−ZP−I shows a biphasic fluorescence decay that has been satisfactorily reproduced by a double exponential formula (Table 2), implying the thermal repopulation of $^1(ZC)*-ZP-I$ from the initial ion pair $(ZC)^+-(ZP)^--I$ in competition with the charge-recombination and charge-shift reactions (Scheme 4b). The biphasic fluorescence decay has been analyzed in essentially the same manner as ZC−ZP using eqs 5−8 with substituting k_{CR1} by $k_{CR1} + k_{CSH}$: we have obtained values of $k_{CS} = 2.3 \times 10^{10}$, $k_{ret} = 2.9 \times 10^9$ s^{-1}, and $k_{CR1} + k_{CSH} = 1.7 \times 10^{10}$ s^{-1}. Assuming k_{CR1} to be the same as that in ZC−ZP, a value of k_{CSH} can be estimated as 6.4×10^9 s^{-1}. The transient absorption spectra of ZC−ZP−I in DMF (Figure 6b) provide evidence for a stepwise electron-transfer sequence as a main route to the secondary ion pair: $^1(ZC)*-ZP-I \rightarrow (ZC)^+-(ZP)^--I \rightarrow (ZC)^+-ZP-(I)^-$. The 450- and 883-nm transient absorptions appear within ca. 30−40 ps and decay with a time constant of ca. 80 ps. Following the decays of these transient absorptions, the 713-nm absorption

due to (I)$^-$ appears with a time constant of ca. 80 ps. The time-profiles of the 450-, 713-, and 883-nm transient absorptions have been simultaneously simulated in the same manner; the difference absorption coefficients at 713 nm are as follows: $\epsilon(^1(ZC)*)$ = 2×10^3, $\epsilon((ZC)^+-(ZP)^-) = 1.0 \times 10^4$, $\epsilon((ZC)^+-ZP-(I)^-)$ = 5.1×10^4, and e($^3(ZC)*$) = 2×10^3 M^{-1} cm^{-1}. As shown in Figure 7, the three time profiles have been nicely reproduced by employing a value of $k_{CSH} = 1.0 \times 10^{10}$ s^{-1}. Except for a somewhat large discrepancy in the estimated value of k_{CS1}, the two analyses gave the similar results. Finally, the quantum yield for the formation of $(ZC)^+-ZP-(I)^-$ has been estimated to be 0.47 on the basis of the absorption data; the amount of $^1(ZC)*$ formed by incident light was determined by the extrapolation of the absorbance at 450 nm to 0 decay time and the amount of $(ZC)^+-ZP-(I)^-$ was determined by the constant absorbance at 713 nm.

In THF, the fluorescence quantum yield of $^1(ZC)*-ZP$ is nearly the same as that of reference $^1(ZC)*$ (Figure 5b), and the fluorescence decay curve has been reproduced by double exponential formula with time constants of 38 ps (33%) and 880 ps (67%). Figure 8a shows the transient absorption spectra of ZC−ZP taken for excitation at 635 nm in THF. By comparing the reference transient absorption spectra of $^1(ZC)*$ and $^3(ZC)*$ (shown as dotted line in Figure 8a), the major spectral changes displayed in Figure 8a can be explained in terms of the intersystem crossing from $^1(ZC)*-ZP$ to $^3(ZC)*-ZP$ occurring with a time constant of ca. 900 ps which is quite similar to that of the reference ZC. However, it is worthy to note that distinct, albeit small, absorbance at 448 nm was observed in the spectra at 40−400-ps delay times, which indicates the formation of a small amount of $(ZC)^+-(ZP)^-$. This absorption rises with a time constant of 55 ps and then decays with a time constant of ca. 1 ns. A possible mechanism accounting for these observation is again an equilibrium between $^1(ZC)*-ZP$ and $(ZC)^+-(ZP)^-$ *but under conditions of $k_0 > k_{CR1}$ and $k_{ret} > k_{CS1}$* (Scheme 5a). By using the respective difference absorption coefficients in THF, $\epsilon(^1(ZC)*)_{450} = 3.9 \times 10^4$, $\epsilon(^1(ZC)*)_{883} = 4.0 \times 10^3$, $\epsilon((ZC)^+-(ZP)^-)_{450} = 1.38 \times 10^5$, $\epsilon((ZC)^+-(ZP)^-)_{883} = 1.6 \times 10^4$, $\epsilon(^3(ZC)*)_{450} = 5.4 \times 10^4$, and $\epsilon(^3(ZC)*)_{883} = 2.0 \times 10^3$ M^{-1} cm^{-1}, the time-profiles at 450 and 883 nm were adequately reproduced with values of $k_0 = 1.3 \times 10^9$, $k_{CS1} = 4.5 \times 10^9$, $k_{CR1} = 2.7 \times 10^8$, and $k_{ret} = 1.3 \times 10^{10}$ s^{-1} (Figure 9). These obtained rates satisfy the above conditions. The energy difference ΔG between $^1(ZC)*$ and $(ZC)^+-(ZP)^-$ has been again determined directly from the relationship $\Delta G = -RT \ln (k_{CS1}/k_{ret})$. This provides the energy
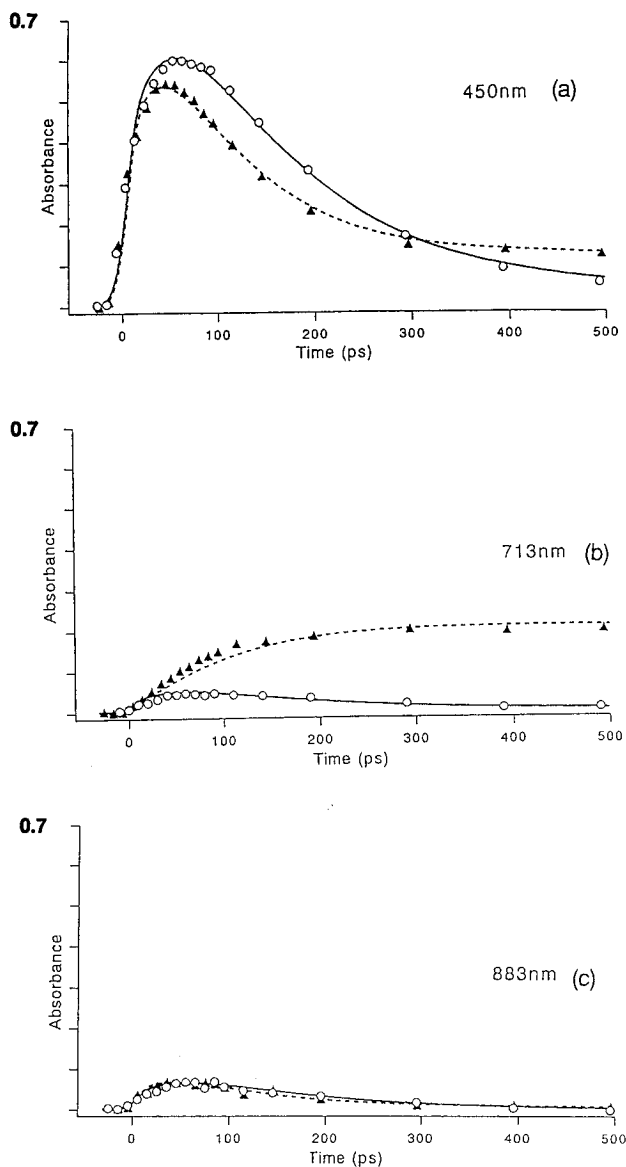
Figure 7. Time profiles in the transient absorption spectra of ZC−ZP (○) and of ZC−ZP−I (▲) in DMF.

of the ion-pair state 0.03 eV above that of ^{1}(ZC)*. On the basis of these results, the energy levels of the ion pair state in THF are corrected in the same manner as in DMF (Table 1).

The fluorescence decay curve of ZC−ZP−I in THF has been reproduced by double exponential formula with time constants of 39 ps (22%) and 217 ps (78%) (Table 2). The transient absorption spectra of ZC−ZP−I in THF (Figure 8b) display clearly the rise of the absorption of (I)$^-$ with a time constant of ca. 210 ps without distinct appearance of the absorption of (ZP)$^-$. At a glance, it looks like a long-distance electron transfer from ^{1}(ZC)* to I provides (ZC)$^+$−ZP−(I)$^-$ directly. In this case again, however, note that the weak absorption around 450 nm characteristic of (ZP)$^-$ appears with $\tau = 18$ ps and decays with $\tau = 230$ ps, although its amplitude is quite small. These observations, along with the results obtained for ZC−ZP, suggest a possible kinetic scheme shown in Scheme 5b, in which the intermediate ion-pair state (ZC)$^+$−(ZP)$^-$−I equilibrated with ^{1}(ZC)*−ZP−I is trapped by a charge-shift reaction to a more stable, secondary ion pair (ZC)$^+$−ZP−(I)$^-$. When k_{CSH} is much larger than k_{CS1}, the detection of (ZC)$^+$−(ZP)$^-$−I will be very difficult. As in the analysis of the data for ZC−ZP, the time profiles at the 450-, 713-, and 883-nm bands have been simultaneously nicely reproduced by employing a value of k_{CSH} = 4.0 × 10^{10} s^{-1} in addition to k_0, k_{CS1}, k_{ret}, and k_{CR1} used for

Scheme 5. Reaction Schemes of ZC−ZP (a) and ZC−ZP−I (b) in THF
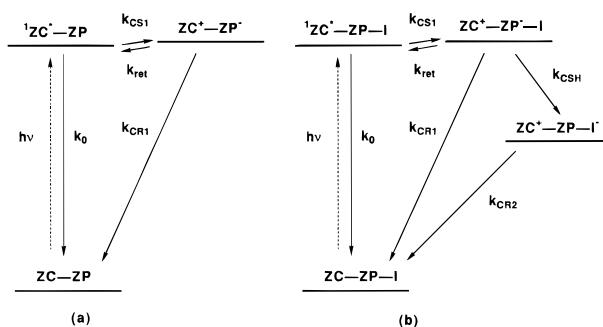
the fit of the ZC−ZP data (Figure 9). As noted, a situation that $k_{CSH} > k_{CS1}$ leads to only small accumulation of (ZC)$^+$−(ZP)$^-$−I, thereby precluding its distinct detection in the transient absorption spectra. The quantum yield for the formation of (ZC)$^+$−ZP−(I)$^-$ has been determined to be as high as 0.90 on the basis of the absorbance of the final ion pair.

Discussion

As described above, the kinetic and spectroscopic data collected for ZC−HP−I and ZC−ZP−I triads reveal a two-step electron-transfer relay with the intermediate ion-pair state, (ZC)$^+$−(HP)$^-$−I or (ZC)$^+$−(ZP)$^-$−I, as a real intermediate for the main pathway leading to the long-lived charge-separated ion-pair states. In detail, however, the two triads follow different reaction schemes; a simple two-step mechanism for ZC−HP−I vs a pre-equilibrium followed by a charge-shift reaction for ZC−ZP−I. These mechanisms are consistent with the energy diagrams estimated for the triads (Table 1). Since the energy levels of the ion-pair states are dependent upon the solvent polarity, the respective electron-transfer rates and thus the overall quantum yield for the formation of the secondary ion pair are quite solvent dependent (Table 3). In ZC−HP−I, both the initial charge separation and the subsequent charge-shift reaction have sufficient driving force to allow the sequential electron-transfer relay where the reverse electron transfer process can be neglected, while in ZC−ZP−I the corresponding energy difference between ^{1}(ZC)*−ZP−I and (ZC)$^+$−(ZP)$^-$−I is much smaller (slightly exothermic in DMF and slightly endothermic in THF) and that for the secondary charge-shift reaction is much larger. Therefore, in the latter system, the reverse process, (ZC)$^+$−(ZP)$^-$−I → ^{1}(ZC)*−ZP−I, must be taken into account.

As the other mechanistic possibility for the formation of the secondary ion pair, one may envision a direct, long-distance electron transfer via a superexchange mechanism. Usually this mechanism becomes important when the energy level of the intermediate ion-pair state is higher than that of the starting excited state. In this case, the intermediate ion-pair state can be used as a virtual state in the superexchange mechanism. According to the formalism developed for the superexchange mechanism,[36] the electronic matrix element, V_s, for the superexchange interaction between states i, m, and n, where i and n are the initial and final states and m is the virtual state, is given by eq 9

$$V_s = V_{mi}V_{nm}/\Delta E_{mi} \qquad (9)$$

where V_{mi} and V_{nm} are the respective electronic interaction matrix elements between the states i and m and m and n, and ΔE_{mi} is the energy difference between the states i and m. In

(35) Very rapid charge recombination ($k_{CR} > 10^{11}$ s^{-1}) has been reported for a related porphyrin−porphyrin ion-pair lying ca. 1.34 eV above the ground state in butyronitrile, ref 15a.

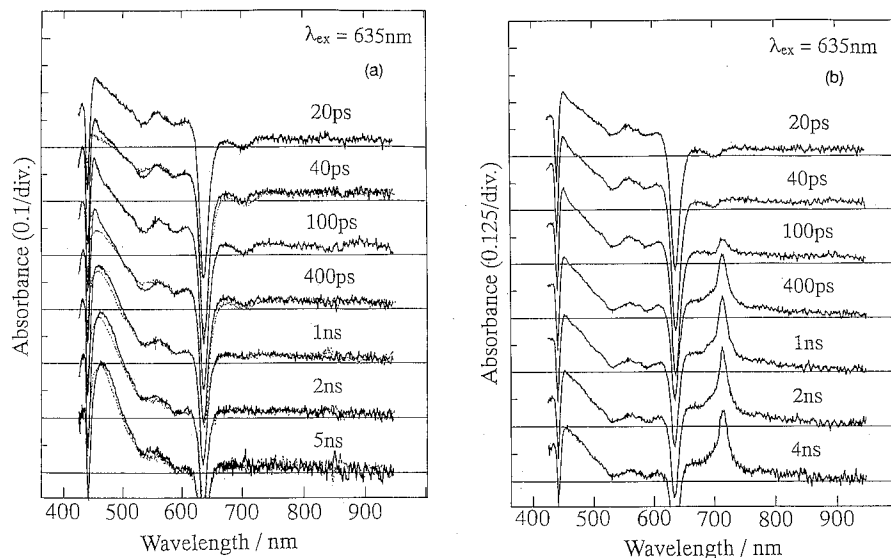(36) Won, Y.; Friesner, R. A. *Biochim. Biophys. Acta* **1988**, *935*, 9.

Figure 8. Time-resolved transient absorption spectra of ZC−ZP (a) and ZC−ZP−I (b) in THF taken for excitation at 635 nm.
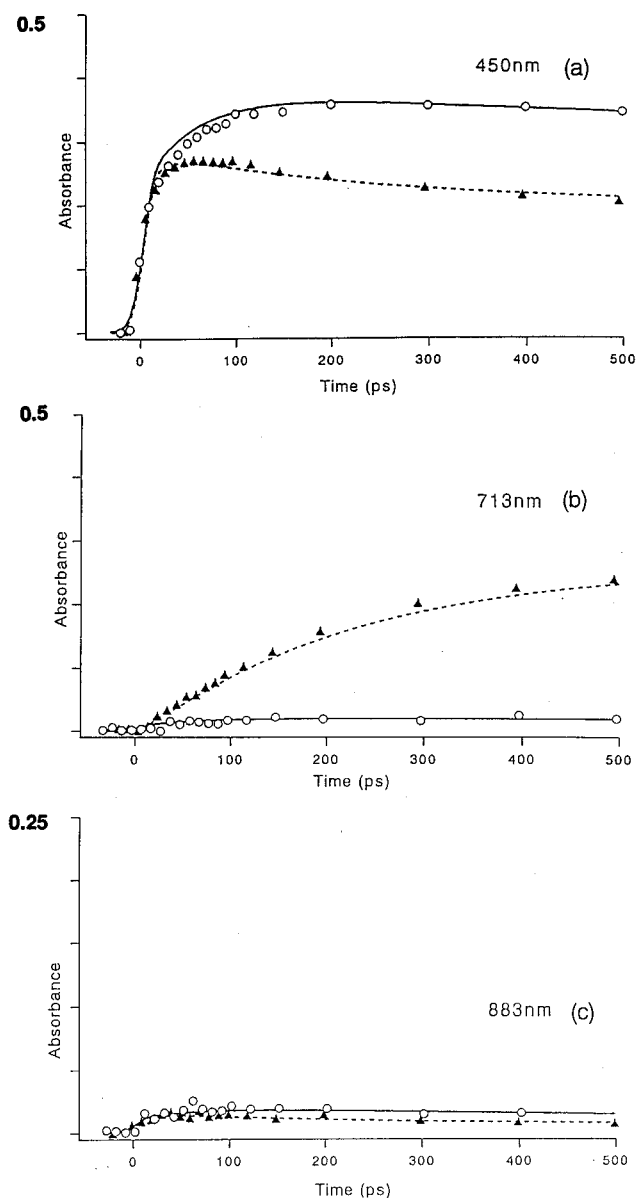

Figure 9. Time profiles in the transient absorption spectra of ZC−ZP (○) and of ZC−ZP−I (▲) in THF.

this case, i = ^{1}(ZC)*−P−I, m = (ZC)$^+$−(P)$^-$−I, and n = (ZC)$^+$−P−(I)$^-$, respectively.

In ZC−HP−I, the energy level of (ZC)$^+$−(HP)$^-$−I is lower than that of ^{1}(ZC)* in THF and DMF. The decay time constants of ^{1}(ZC)*−HP−I determined by their fluorescence lifetime and the transient absorption data are quite similar to those of ^{1}(ZC)*−HP. These facts strongly imply the unimportance of the superexchange-mediated long distance electron transfer in ZC−HP−I. On the other hand, the energy of (ZC)$^+$−(ZP)$^-$−I has been estimated to be slightly higher than that of ^{1}(ZC)* in THF. The estimated small ΔE_{mi} might encourage the super-exchange-mediated, single-step electron transfer in ZC−ZP−I. However, the observation of the transient absorption due to (ZP)$^-$ conflicts with the single-step mechanism. As described above, the kinetic traces of the transient absorbances can be nicely reproduced by considering the pre-equilibrium mechanism (Schemes 4b and 5b). Therefore, we conclude that the contribution of the superexchange-mediated electron transfer is small, if present, and its rate will be much smaller than the rate of the electron transfer by the sequential mechanism. In the superexchange mechanism, the electronic coupling between the initial and final states through the intermediate state must be coherent. Namely, the superexchange electron transfer must be sufficiently rapid in order to avoid the relaxation of the intermediate state caused by the dynamic environmental per-turbations (solvation dynamics) which will take place within a few picoseconds in the solvents used here at room temperature. In this respect, the magnitudes of the matrix elements V_{mi} and V_{nm} in eq 9 in the present models do not seem to be sufficiently larger for the superexchange electron transfer. These reasonings concerning the superexchange mechanism on the basis of these experimental results are supported by detailed theoretical studies on the superexchange and sequential electron transfer mecha-nisms.[37]

The charge recombination reactions of the intermediate ion-pair states, (ZC)$^+$−(HP)$^-$−I and (ZC)$^+$−(ZP)$^-$−I, to the ground state are rapid in polar DMF,[35] which leads to small overall quantum yields for the secondary ion-pair states. This feature, which has also been found for porphyrin−quinone,[29] porphyrin−pyromellitimide,[11] and other dyads,[31] notes the importance of a relatively nonpolar environment in slowing down the undesirable charge recombination. In addition, of course, $k_{CR1} \ll k_{CSH}$ must be a key condition for the high quantum yield of the secondary ion-pair state. Here it is interesting to note that a clear-cut, direct detection of a charge-shift reaction of (P$_1$)$^+$−(P$_2$)$^-$−A

(37) Sumi, H., private communication. N.M. is grateful to Dr. Sumi for his helpful discussions.

Table 3. Electron Transfer Rate Constants[a] Determined for ZC−HP−I and ZC−ZP−I

	k_{CS1}	k_{CR1}	k_{CSH}	k_{ret}	ϕ^b	k_{CR2}
			ZC−HP−I			
DMF	9.9×10^{10}	3.3×10^{10}	2.4×10^9		0.07	5.0×10^6
$\Delta G^{0\ c}$	-0.31	-1.63	-0.37			-1.26
THF	4.9×10^{10}	2.5×10^9	5.8×10^9		0.70	$2.5 \times 10^6\ (0.42),^d\ 9.0 \times 10^6\ (0.52)^d$
$\Delta G^{0\ c}$	-0.23	-1.71	-0.22			-1.49
			ZC−ZP−I			
DMF	1.4×10^{10}	1.1×10^{10}	1.0×10^{10}	2.4×10^9	0.47	4.2×10^6
$\Delta G^{0\ c}$	-0.05	-1.89	-0.63	0.05		-1.26
THF	4.5×10^9	2.7×10^8	4.0×10^{10}	1.3×10^{10}	0.90	$2.7 \times 10^6\ (0.30),^d\ 7.9 \times 10^9\ (0.70)^d$
$\Delta G^{0\ c}$	0.03	-1.97	-0.48	-0.03		-1.49

[a] Determined on the basis of the transient absorption spectroscopy. Unimolecular rate, s^{-1}. [b] The overall quantum yield for formation of $(ZC)^+-P-(I)^-$. [c] The energy gaps (ΔG^0) are calculated on the basis of the corrected energy levels, eV. [d] Pre-exponential factor in biexponential fit.

to $(P_1)^+-P_2-(A)^-$ is quite rare, regardless of its crucial importance in practical design of multicomponent artificial models. Although only limited points are available, the increase of the energy gap results in the increase in k_{CSH} both in THF and DMF, and the solvent polarity dependence seems to be rather small. This tendency is also observed in charge separation reaction of distance-fixed donor−acceptor pairs and is expected from the parallel increase of the reorganization energy and the energy gap with increase of the solvent polarity. These features are quite similar to those found for a charge shift reaction in porphyrin−pyromellitimide−quinone triads.[14]

In summary, the large transient absorption bands of $(I)^-$, $(HP)^-$, and $(ZP)^-$ are informative particularly with regard to the assignment of ionic states and thus the excited-state dynamics. By analyzing the time-dependence of these signals, we can reveal the whole electron transfer sequences in these rather complicated molecular systems. In these triads, the ZC moiety is quite similar to the special pair in its dual functions as an efficient singlet energy sink as well as the first electron donor to nearby HP or ZP. It has been clearly shown by the picosecond transient absorption spectroscopy that ZC−HP−I undergoes a two-step electron-transfer relay, $^1(ZC)^*-HP-I \rightarrow (ZC)^+-(HP)^--I \rightarrow (ZC)^+-HP-(I)^-$, whereas ZC−ZP−I follows a different reaction scheme involving an equilibrium between $^1(ZC)^*-ZP-I$ and $(ZC)^+-(ZP)^--I$ accompanied by a rapid charge shift reaction to give $(ZC)^+-ZP-(I)^-$.

The rational molecular design of photosynthetic models needs a very detailed knowledge of effects of structural and environmental perturbations on the reaction mechanisms of the triads. On the basis of these results as well as the earlier ones, we are approaching mimicry of the natural photosynthetic charge separation. Further works directed toward achieving these goals are current underway in our laboratories.

Experimental Section

All commercially available reagents and solvents were used without further purification unless otherwise stated. Acetonitrile and dichloromethane were refluxed over and distilled from P_2O_5. Pyridine was distilled and stored over KOH. Preparative separations were usually performed by flash column chromatography on silica gel (Merck, Kieselgel 60H, Art. 7736; Wako pure chemical industries LTD, Wakogel, C-200).

^{1}H-NMR spectra were recorded on a JEOL α-500 spectrometer (operating as 500 MHz), and chemical shifts were represented as δ-values relative to the internal standard TMS. UV−visible spectra were recorded on a Shimadzu UV-3000 spectrometer, and steady-state fluorescence spectra were taken on a Shimadzu RF-502A spectrofluorimeter. High resolution mass spectra (HRMS) were recorded on a JEOL HX-110 mass spectrometer. PEG (polyethyleneglycol) or CsI was used as the internal standards. *m*-Nitrobenzyl alcohol was used as the FAB (fast atom bombardment) matrix, and the positive FAB ionization method was used at accelerating voltage 10 kV with Xe atom

as the primary ion source. IR spectra (KBr method) were taken on a HORIBA FT-3000 spectrometer.

Fluorescence lifetimes were measured on 10^{-7} M solutions with a picosecond time-correlated single-photon counting system.[38] The fluorescence lifetimes of ZC have been determined by measuring the 640-nm emission for excitation at 620 nm, and those of ZP have been determined by measuring the 590-nm for excitation at 532 nm. Picosecond transient absorption spectra were measured by means of a microcomputer-controlled double-beam picosecond spectrometer with a picosecond dye laser 8-ps pulse duration pumped by the second harmonic of a repetitive mode-locked Nd^{3+}:YAG laser.[39] The 635-nm output of the dye laser was used for excitation. Nanosecond transient absorption spectra were taken with the second harmonic output 532 nm of a Q-switched Nd^{3+}:YAG laser (Quantel YG 580, fwhm; 8 ns) was used to excite the model compound. Solutions of the triad compounds (ca. 10^{-5} M) were deaerated by bubbling with argon. Nanosecond-transient absorption changes of the excited solution were measured using a spectrograph (CT-25C, Japan Spectroscopic Co., Ltd.) equipped with a grating blazed at 1000 nm and with a photomultiplier R3896 (Hamamatsu Photonics). The photocurrent was amplified with a wide-band width amplifier, CLC140 (Comlinear, DC-600 MHz). The details of data-acquicition have been described elsewhere.[40]

Determination of the molecular extinction coefficients was done as follows. $\epsilon(^1(ZC)^*)$ and $\epsilon(^3(ZC)^*)$ were determined by (1) comparing the absorbance at certain wavelength with the intensity of the Qy-bleaching around 635 nm where the molecular extinction coefficient of the ground state is known (5.1×10^5 in THF and 5.4×10^4 M^{-1} s^{-1} in DMF), and (2) such values were normalized to the absorbance of the ground-state absorption spectrum where a 0-cross-point was observed in the transient spectrum. At the 0-cross-point, ϵ of the ground state should be the same as that of the excited states. $\epsilon(^1(ZC)^*)$ was determined on the basis of the transient spectrum at 40-ps delay time, and $\epsilon(^3(ZC)^*)$ was determined on the basis of the transient spectrum at 2-ns delay time. $\epsilon((ZC)^+-(HP)^-)$ was determined essentially in the same manner by using the transient spectrum at 200-ps delay time under an assumption of $\Phi((ZC)^+-(HP)^-) = 1$. Contribution by $\epsilon(^1(ZC)^*)$ or $\epsilon(^3(ZC)^*)$ was neglected since the charge separation was complete. $\epsilon((ZC)^+-P-(I)^-)$ was determined essentially in the same manner by using the transient spectrum at 2-ns delay time. The determined values here were quite similar to those reported previously.[14] $\epsilon((ZC)^+-(ZP)^-)$ could not be determined by the above methods since the ion-pair state is equilibrated with the excited state. Thus we attempted to reproduce the kinetic traces by changing these values as variables. The estimated values were found to be quite similar to those of (Zn-TPP),[41] implying the validity of these estimates.

Synthesis of 4. The dipyrrylmethane **2** (7.32 g, 28.3 mmol) and the aldehydes **1** (2.53 g, 14.2 mmol) and **3** (3.12 g, 14.2 mmol) were dissolved in acetonitrile (100 mL). Trichloroacetic acid (TCA) (1.16 g, 14.2 mmol) was added to this solution, and the mixture was stirred for 9 h at room temperature under N_2 atmosphere in the dark. A

(38) Yamazaki, I.; Tamai, N.; Kume, H.; Tsuchiya, H.; Oba, K. *Rev. Sci. Instrum*. **1985**, *56*, 1187.

(39) Hirata, Y.; Mataga, N. *J. Phys. Chem.* **1991**, *95*, 1640.

(40) Nozaki, K.; Ohno, T.; Haga, M. *J. Phys. Chem.* **1992**, *96*, 10880.

(41) Felton, R. H. In *The Porphyrins*, *Vol. 5*; Dolphin, D., Ed.; Academic Press: 1978; p 73.

solution of *p*-chloranil (6.96 g, 28.3 mmol) in THF (200 mL) was added, and the solution was stirred for an additional 6 h. After evaporation of the solvent, the residue was dissolved in CH_2Cl_2 (500 mL), and the resultant solution was successively treated with 3 N HCl (400 mL) and aqueous Na_2CO_3 (400 mL) and then dried over anhydrous Na_2SO_4. After usual metalation with $Zn(OAc)_2$, the porphyrin products were roughly separated by column chromatography on silica gel (Wakogel C-200, CH_2Cl_2 eluent). The reddish porphyrin fraction was collected, and the solvent was evaporated. For easier separation of the porphyrin products, the acetal was once deprotected. Thus, trifluoroacetic acid (TFA) (50 mL) and 10% H_2SO_4 (50 mL) were added to a solution of the porphyrin mixture in $CHCl_3$ (200 mL), and the resultant mixture was refluxed for 20 h. After being cooled, the solution was neutralized with aqueous Na_2CO_3, and the organic solvent was evaporated. The residue was separated by flash column chromatography on silica gel (CH_2Cl_2 eluent). The second fraction that contained the desired porphyrin was collected. Formyl substituted porphyrin (2.98 g, 3.85 mmol) thus obtained was again heated in the presence of 2,2-dimethyl-1,3-propanediol (440 mg, 4.23 mmol) and *p*-toluenesulfonic acid monohydrate (1.61 g, 8.46 mmol) in benzene (300 mL). The mixture was refluxed for 6 h, poured into aqueous Na_2CO_3, and dried over anhydrous Na_2SO_4. After evaporation of the solvent, recrystallization from CH_2Cl_2/MeOH gave **4** as violet crystals (3.30 g, 3.83 mmol) in 27% yield based on the amount of **3** used.

4: mp >300 °C; ^{1}H-NMR ($CDCl_3$) −1.90 (br, 2H, NH), 0.92 (s, 3H, Me), 1.17 (t, 6H, $J = 7.3$ Hz, Et), 1.19 (t, 6H, $J = 7.3$ Hz, Et), 1.46 (s, 3H, Me), 1.84 (t, 6H, $J = 7.3$ Hz, Et), 1.86 (t, 6H, $J = 7.9$ Hz, Et), 2.78 (q, 4H, $J = 7.3$ Hz, Et), 3.03 (q, 4H, $J = 7.3$ Hz, Et), 3.52 (s, 6H, OMe), 3.84 (d, 2H, $J = 11.0$, CH_2), 3.96 (d, 2H, $J = 11.0$, CH_2), 3.99 (q, 4H, $J = 7.3$ Hz, Et), 4.01 (q, 4H, $J = 7.9$ Hz, Et), 5.75 (s, 1H, CH), 6.94 (d, 2H, $J = 8.6$ Hz, Ar-H), 7.74 (t, 1H, $J = 8.6$ Hz, Ar-H), 7.79 (d, 2H, $J = 7.6$ Hz, Ar-H), 8.20 (d, 2H, $J = 7.6$ Hz, Ar-H), 10.18 (s, 2H, meso-H); HRMS (FAB) found, m/z 861.5310; calcd for $C_{56}H_{68}O_4N_4$, m/z 861.5320 ($M^+ + H$).

Synthesis of 5. The synthesis of oxochlorins **5** was carried out by a modified Chang's method.[26] Dry pyridine (0.11 mL) was added to a dry ether (5.0 mL) solution of OsO_4 (1.0 g, 3.93 mmol). The resultant yellow solution of OsO_4−pyridine complex was added to a solution of the porphyrin **4** (960 mg, 1.11 mmol) in dry CH_2Cl_2 (50 mL). The mixture was stirred for 24 h at room temperature under a dry Ar atmosphere in the dark. H_2S gas was passed through the mixture for 1 h so as to induce the precipitation of osmium sulfide. The resultant precipitate was filtered off. TFA (30 mL) and 10% H_2SO_4 (30 mL) were added to the filtrate. The resulting solution was refluxed for 24 h, and the reaction mixture was poured into water. The organic layer was separated, successively washed with water and aqueous Na_2CO_3, and dried over anhydrous Na_2SO_4. After evaporation of the solvent, the oxochlorin isomers were separated by silica gel flash column chromatography (MeOH−free CH_2Cl_2 eluent). Each isomer was precipitated from CH_2Cl_2/hexane, giving **5a** (220 mg, 0.28 mmol, 25% yield) and **5b** (130 mg, 0.16 mmol, 15% yield), respectively.

5a: mp >300 °C; ^{1}H-NMR ($CDCl_3$); −1.65 (s, 1H, NH), −0.81 (br, 1H, NH), 0.27 (t, 6H, rearranged-Et), 1.13 (t, 3H, $J = 7.3$ Hz, Et), 1.16 (t, 3H, $J = 7.3$ Hz, Et), 1.18 (t, 3H, $J = 7.3$ Hz, Et), 1.77 (t, 3H, $J = 7.3$ Hz, Et), 1.80 (t, 3H, $J = 7.3$ Hz, Et), 1.85 (t, 3H, $J = 7.3$ Hz, Et), 2.12 (m, 4H, rearranged-Et), 2.66 (q, 2H, $J = 7.3$ Hz, Et), 2.87 (q, 2H, $J = 7.3$ Hz, Et), 3.03 (q, 2H, $J = 7.3$ Hz, Et), 3.55 (s, 6H, OMe), 3.84 (q, 2H, $J = 7.3$ Hz, Et), 3.98 (q, 2H, $J = 7.3$ Hz, Et), 4.00 (q, 2H, $J = 7.3$ Hz, Et), 6.95 (d, 2H, $J = 8.5$ Hz, Ar-H), 7.75 (t, 1H, $J = 8.5$ Hz, Ar-H), 8.19 (d, 2H, $J = 7.9$ Hz, Ar-H), 8.25 (d, 2H, $J = 7.9$ Hz, Ar-H), 9.95 (s, 1H, meso-H), 10.02 (s, 1H, meso-H), 10.36 (s, 1H, CHO); HRMS (FAB) found, m/z 791.4497; calcd for $C_{51}H_{58}O_4N_4$, m/z 791.4537 ($M^+ + H$); IR (KBr) ν_{max} 1707 cm^{-1} (CHO, CO).

5b: mp 274−275 °C; ^{1}H-NMR ($CDCl_3$); 1.75 (s, 1H, NH, the other peak of NH was not detected), 0.30 (t, 6H, rearranged-Et), 1.11 (t, 3H, $J = 7.3$ Hz, Et), 1.17 (t, 3H, $J = 7.3$ Hz, Et), 1.19 (t, 3H, $J = 7.3$ Hz, Et), 1.76 (t, 3H, $J = 7.3$ Hz, Et), 1.77 (t, 3H, $J = 7.3$ Hz, Et), 1.82 (t, 3H, $J = 7.3$ Hz, Et), 2.58 (m, 4H, rearranged-Et), 2.83 (q, 2H, $J = 7.3$ Hz, Et), 2.88 (q, 2H, $J = 7.3$ Hz, Et), 3.02 (q, 2H, $J = 7.3$ Hz, Et), 3.57 (s, 6H, OMe), 3.83 (q, 2H, $J = 7.3$ Hz, Et), 3.89 (q, 2H, $J = 7.3$ Hz, Et), 3.99 (q, 2H, $J = 7.3$ Hz, Et), 6.95 (d, 2H, $J = 8.5$ Hz, Ar-H), 7.76 (t, 1H, $J = 8.5$ Hz, Ar-H), 8.08 (d, 2H, $J = 7.9$ Hz, Ar-H), 8.21 (d, 2H, $J = 7.9$ Hz, Ar-H), 9.06 (s, 1H, meso-H), 10.04 (s, 1H, meso-

H), 10.33 (s, 1H, CHO); HRMS (FAB) found, m/z 791.4571; calcd for $C_{51}H_{58}O_4N_4$, m/z 791.4537 ($M^+ + H$); IR (KBr) ν_{max} 1745 cm^{-1} (CHO), 1707 cm^{-1} (CO).

Synthesis of 6. The oxochlorin **5a** (220 mg, 0.28 mmol), 2,2-dimethyl-1,3-propanediol (29 mg, 0.28 mmol), and *p*-toluenesulfonic acid monohydrate (265 mg, 1.40 mmol) were dissolved in benzene (100 mL). The mixture was refluxed for 6 h, and poured into aqueous Na_2CO_3, and dried over anhydrous Na_2SO_4. After evaporation of the solvent, oxochlorin **6** was purified by silica gel flash column chromatography (benzene eluent). Precipitation from CH_2Cl_2/Hexane gave **6** as violet crystals (186 mg, 0.21 mmol) in 76% yield.

6: mp 225−227 °C; ^{1}H-NMR ($CDCl_3$) −1.68 (s, 1H, NH), −0.82 (br, 1H, NH), 0.25 (t, 6H, rearranged-Et), 0.92 (s, 3H, Me), 1.12 (t, 3H, $J = 7.3$ Hz, Et), 1.16 (t, 3H, $J = 7.3$ Hz, Et), 1.18 (t, 3H, $J = 7.3$ Hz, Et), 1.46 (s, 3H, Me), 1.77 (t, 3H, $J = 7.3$ Hz, Et), 1.80 (t, 3H, $J = 7.3$ Hz, Et), 1.84 (t, 3H, $J = 7.3$ Hz, Et), 2.16 (m, 4H, rearranged-Et), 2.65 (q, 2H, $J = 7.3$ Hz, Et), 2.86 (q, 2H, $J = 7.3$ Hz, Et), 3.02 (q, 2H, $J = 7.3$ Hz, Et), 3.54 (s, 6H, OMe), 3.83 (d, 2H, $J = 11.0$ Hz, CH_2), 3.84 (q, 2H, $J = 7.3$ Hz, Et), 3.95 (d, 2H, $J = 11.0$ Hz, CH_2), 3.98 (q, 4H, $J = 7.3$ Hz, Et), 5.71 (s, 1H, CH), 6.93 (d, 2H, $J = 8.5$ Hz, Ar-H), 7.74 (t, 1H, $J = 8.5$ Hz, Ar-H), 7.78 (d, 2H, $J = 7.9$ Hz, Ar-H), 8.04 (d, 2H, $J = 7.9$ Hz, Ar-H), 9.94 (s, 1H, meso-H), 9.99 (s, 1H, meso-H); HRMS (FAB) found, m/z 877.5281; calcd for $C_{56}H_{68}O_5N_4$, m/z 877.5279 ($M^+ + H$); IR (KBr) ν_{max} 1712 cm^{-1} (CO).

Synthesis of 7. MeLi (as complex of LiBr) (1.5 M) solution in ether (0.82 mL, 1.23 mmol) was added to a solution of the oxochlorin **6** in dry ether (20 mL). The mixture was stirred at room temperature under N_2 atmosphere. Progress of the reaction was monitored by TLC every 15 min. After confirming a nearly complete conversion of the starting material, the reaction was stopped by addition of water. Normally, it took ca. 90 min. Excess reaction time often led to a drastic decrease of the product yield. The reaction mixture was poured into water. The organic layer was separated and dried over anhydrous Na_2SO_4. After evaporation of the solvent, the residue was separated by flash column chromatography on silica gel (CH_2Cl_2/Et_2O (99/1) eluent). Hydroxychlorin **7** was eluted as dark violet band. This fraction was collected, and the solvent was evaporated. Precipitation from CH_2Cl_2/hexane gave **7** (125 mg, 0.10 mmol) in 57% yield.

7: mp 205−207 °C; ^{1}H-NMR ($CDCl_3$) −0.95 (s, 1H, NH), −0.07 (br, 1H, NH), 0.02 (t, 3H, rearranged-Et), 0.90 (s, 3H, Me), 0.94 (t, 3H, rearranged-Et), 1.08 (t, 3H, Et), 1.09 (t, 3H, Et), 1.13 (t, 3H, Et), 1.44 (s, 3H, Me), 1.60 (m, 1H, Et), 1.71 (t, 6H, Et), 1.75 (t, 3H, Hz, Et), 1.83 (m, 1H, Et), 1.90 (s, 3H, Me), 2.16 (m, 1H, Et), 2.24 (m, 1H, Et), 2.37 (m, 1H, Et), 2.59 (m, 1H, Et), 2.78 (s, 1H, OH), 2.79 (m, 2H, Et), 2.95 (m, 2H, Et), 3.52 (s, 3H, OMe), 3.57 (s, 3H, OMe), 3.76 (q, 2H, Et), 3.81 (d, 2H, $J = 11.0$ Hz, CH_2), 3.81 (q, 2H, Et), 3.88 (q, 1H, Et), 3.88 (q, 1H, Et), 3.93 (d, 2H, $J = 11.0$ Hz, CH_2), 5.68 (s, 1H, CH), 6.89 (d, 1H, $J = 8.6$ Hz, Ar-H), 6.91 (d, 1H, $J = 8.6$ Hz, Ar-H), 7.65 (dd, 1H, $J = 7.9$, 1.5 Hz, Ar-H), 7.68 (dd, 1H, $J = 7.9$, 1.5 Hz, Ar-H), 7.70 (t, 1H, $J = 8.6$ Hz, Ar-H), 7.73 (dd, 1H, $J = 7.9$, 1.5 Hz, Ar-H), 8.18 (dd, 1H, $J = 7.9$, 1.5 Hz, Ar-H), 9.04 (s, 1H, meso-H), 9.82 (s, 1H, meso-H); HRMS (FAB) found, m/z 893.5597; calcd for $C_{57}H_{72}O_5N_4$ 893.5582 ($M^+ + H$); IR (KBr) ν_{max} 3454 cm^{-1} (OH).

Synthesis of 8. The hydroxychlorin **7** (96 mg, 0.11 mmol) and 2,2-dimethyl-1,3-propanediol (11 mg, 0.11 mmol) were dissolved in benzene (50 mL). TFA (0.96 mL) was added to this solution, and the mixture was refluxed for 6 h. The reaction mixture was poured into water and extracted with CH_2Cl_2. The organic layer was separated, successively washed with aqueous Na_2CO_3, and dried over anhydrous Na_2SO_4. After evaporation of the solvent, the product was separated by silica gel flash column chromatography (CH_2Cl_2/Et_2O (98/2) eluent). The dark brown band was collected, and the solvent was evaporated. Precipitation from CH_2Cl_2/hexane gave **8** (79 mg, 0.09 mmol) in 84% yield.

8: mp 284−285 °C; ^{1}H-NMR ($CDCl_3$) −1.68 (s, 1H, NH, the other peak of NH was not detected), 0.33 (t, 6H, rearranged-Et), 0.91 (s, 3H, Me), 1.07 (t, 3H, $J = 7.3$ Hz, Et), 1.10 (t, 3H, $J = 7.3$ Hz, Et), 1.11 (t, 3H, $J = 7.3$ Hz, Et), 1.46 (s, 3H, Me), 1.70 (m, 2H, rearranged-Et), 1.71 (t, 3H, $J = 7.3$ Hz, Et), 1.77 (t, 6H, $J = 7.3$ Hz, Et), 2.23 (m, 2H, rearranged-Et), 2.48 (q, 2H, $J = 7.3$ Hz, Et), 2.81 (q, 2H, $J = 7.3$ Hz, Et), 2.97 (q, 2H, $J = 7.3$ Hz, Et), 3.54 (s, 6H, OMe), 3.78 (q, 2H, $J = 7.3$ Hz, Et), 3.80 (d, 2H, $J = 11.0$ Hz, CH_2), 3.87 (q, 2H, $J = 7.3$ Hz, Et), 3.90 (q, 2H, $J = 7.3$ Hz, Et), 3.95 (d, 2H, $J = 11.0$ Hz, CH_2),

5.45 (s, 1H, methylene-CH_2), 5.70 (s, 1H, CH), 6.78 (s, 1H, methylene-CH_2), 6.91 (d, 2H, $J = 8.6$ Hz, Ar-H), 7.71 (t, 1H, $J = 8.6$ Hz, Ar-H), 7.71 (d, 2H, $J = 8.0$ Hz, Ar-H), 8.05 (d, 2H, $J = 8.0$ Hz, Ar-H), 9.54 (s, 1H, meso-H), 9.84 (s, 1H, meso-H); HRMS (FAB): found, m/z 875.5459; calcd for $C_{57}H_{70}O_4N_4$, m/z 875.5476 ($M^+ + H$); IR (KBr) ν_{max} 1653 cm^{-1} (methylene-CH_2).

Synthesis of 9. TFA (8 mL) and 10% H_2SO_4 (8 mL) were added to a solution of methylenechlorin **8** (79 mg, 0.09 mmol) in $CHCl_3$ (30 mL). The solution was refluxed for 6 h and poured into water. The organic layer was separated, successively washed with water and aqueous Na_2CO_3, and dried over anhydrous Na_2SO_4. After evaporation of the solvent, the product was separated by silica gel flash column chromatography (CH_2Cl_2 eluent). The dark brown band was collected; and the solvent was evaporated. Precipitation from CH_2Cl_2/hexane gave **9** (72 mg, 0.09 mmol) in 92% yield.

9; mp 276−278 °C; ^{1}H-NMR ($CDCl_3$) −1.26 (s, 1H, NH), −0.20 (s, 1H, NH), 0.36 (t, 6H, rearranged-Et), 1.10 (t, 3H, $J = 7.3$ Hz, Et), 1.11 (t, 3H, $J = 7.3$ Hz, Et), 1.14 (t, 3H, $J = 7.3$ Hz, Et), 1.73 (t, 3H, $J = 7.3$ Hz, Et), 1.76 (m, 2H, rearranged-Et), 1.80 (t, 6H, $J = 7.3$ Hz, Et), 2.12 (m, 2H, rearranged-Et), 2.51 (q, 2H, $J = 7.3$ Hz, Et), 2.81 (q, 2H, $J = 7.3$ Hz, Et), 2.98 (q, 2H, $J = 7.3$ Hz, Et), 3.55 (s, 6H, OMe), 3.79 (q, 2H, $J = 7.3$ Hz, Et), 3.91 (q, 2H, $J = 7.3$ Hz, Et), 3.93 (q, 2H, $J = 7.3$ Hz, Et), 5.47 (s, 1H, methylene-CH_2), 6.82 (s, 1H, methylene-CH_2), 6.92 (d, 2H, $J = 8.5$ Hz, Ar-H), 7.72 (t, 1H, $J = 8.5$ Hz, Ar-H), 8.12 (d, 2H, $J = 7.9$ Hz, Ar-H), 8.25 (d, 2H, $J = 7.9$ Hz, Ar-H), 9.55 (s, 1H, meso-H), 9.88 (s, 1H, meso-H), 10.34 (s, 1H, CHO); HRMS (FAB) found, m/z 789.4740; calcd for $C_{52}H_{60}O_3N_4$, m/z 789.4744 ($M^+ + H$); IR (KBr) ν_{max} 1703 cm^{-1} (CHO), 1655 cm^{-1} (methylene-CH_2).

Synthesis of ZC−HP−I and ZC−ZP−I. The dipyrrylmethane **10** (88 mg, 599 μmol), methylenechlorin **9** (43 mg, 54.5 μmol), and pyromellitimide-linked aldehyde **11** (288 mg, 545 μmol) were dissolved in dry CH_2Cl_2 (100 mL). TFA (38 μL) (55 mg, 0.49 mmol) was added to this solution, and the mixture was stirred for 24 h at room temperature under N_2 atmosphere in the dark. 2,3-Dichloro-5,6-dicyano-*p*-benzoquinone (DDQ) (177 mg, 0.78 mmol) was added, and the resulting solution was stirred for an additional 12 h. The reaction was quenched with triethylamine (0.5 mL). After evaporation of the solvent, the residue was separated by flash column chromatography on silica gel (CH_2Cl_2 eluent). The brown band was collected, and the solvent was evaporated. Recrystallization from CH_2Cl_2/hexane gave free-base **12** (HC−HP−I, 40 mg, 27.4 μmol) in 51% yield based on the amount of **9** used. ZC−HP−I and ZC−ZP−I were prepared as follows. A saturated methanol solution of $Zn(OAc)_2$ (0.5 mL) was added to a solution of **12** (51.3 mg, 35.2 μmol) in dry CH_2Cl_2 (20 mL). The mixture was stirred at room temperature under N_2 atmosphere. This metalation reaction should be stopped before the complete metalation to ZC−HP−I. Usually, after 30 min stirring, the reaction mixture was poured into water and washed with water. The organic layer was dried over anhydrous Na_2SO_4, and the solvent was evaporated. The residue was separated by flash column chromatography on silica gel (CH_2Cl_2 eluent). The first and second violet fractions contained ZC−HP−I and ZC−ZP−I, respectively. After evaporation of the solvent, precipitation from CH_2Cl_2/hexane yielded ZC−HP−I (7.2 mg, 4.75 μmol, 13%) and ZC−ZP−I (25.7 mg, 16.2 μmol, 46%), respectively.

12 (HC−HP−I): mp 280−282 °C; ^{1}H-NMR ($CDCl_3$) −3.16 (br, 1H, Por-NH), −3.06 (br, 1H, Por-NH), −1.11 (s, 1H, Ch1-NH), −0.13 (br, 1H, Ch1-NH), 0.60 (t, 6H, rearranged-Et), 0.88 (t, 3H, hexyl-Me), 1.14 (t, 3H, $J = 7.3$ Hz, Et), 1.18 (t, 3H, $J = 7.3$ Hz, Et), 1.30 (m, 6H, hexyl-CH_2), 1.60 (m, 2H, hexyl-CH_2), 1.66 (t, 3H, $J = 7.3$ Hz, Et), 1.79 (t, 3H, $J = 7.3$ Hz, Et), 1.85 (t, 3H, $J = 7.3$ Hz, Et), 1.96 (t, 3H, $J = 7.3$ Hz, Et), 2.14 (m, 2H, rearranged-Et), 2.79 (m, 2H, rearranged-Et), 2.86 (q, 2H, $J = 7.3$ Hz, Et), 3.03 (q, 2H, $J = 7.3$ Hz, Et), 3.23 (q, 2H, $J = 7.3$ Hz, Et), 3.51 (t, 2H, hexyl-CH_2), 3.58 (s, 6H, OMe), 3.86 (q, 2H, $J = 7.3$ Hz, Et), 3.96 (q, 2H, $J = 7.3$ Hz, Et), 4.13 (q, 2H, $J = 7.3$ Hz, Et), 5.26 (s, 2H, benzyl-CH_2), 5.68 (s, 1H, methylene-CH_2), 6.94 (d, 2H, $J = 8.6$ Hz, Ar-H), 6.96 (s, 1H, methylene-CH_2), 7.74 (t, 1H, $J = 8.6$ Hz, Ar-H), 7.97 (d, 2H, $J = 7.9$ Hz, Ar-H), 8.02 (s, 2H, Im-Ar-H), 8.34 (d, 2H, $J = 7.9$ Hz, Ar-H), 8.48 (s, 4H, Ar-H), 9.04 (d, 1H, $J = 4.3$ Hz, Por-β-H), 9.06 (d, 1H, $J = 4.3$ Hz, Por-β-H), 9.40 (d, 2H, $J = 4.3$ Hz, Por-β-H), 9.42 (d, 1H, $J = 4.3$ Hz, Por-β-H), 9.49 (d, 1H, $J = 4.3$ Hz, Por-β-H), 9.57 (d, 1H, $J = 4.3$ Hz, Por-β-H), 9.59 (d, 1H, $J = 4.3$ Hz, Por-β-H), 9.68 (s, 1H, Ch1-meso-H), 9.99 (s, 1H, Ch1-meso-H), 10.39 (s, 1H, Por-meso-H), 10.41 (s, 1H, Por-meso-

H); HRMS (FAB) found, m/z 1458.7313; calcd for $C_{94}H_{92}O_6N_{10}$, m/z 1458.7312 ($M^+ + H$); IR (KBr) ν_{max} 1626 cm^{-1} (methylene-CH_2), 1720 cm^{-1} (CO).

ZC−HP−I: mp >300 °C; ^{1}H-NMR ($CDCl_3$) −3.14 (br, 1H, Por-NH), −3.06 (br, 1H, Por-NH), 0.63 (t, 6H, rearranged-Et), 0.88 (t, 3H, Hexyl-Me), 1.10 (t, 3H, $J = 7.3$ Hz, Et), 1.10 (t, 3H, $J = 7.3$ Hz, Et), 1.31 (m, 6H, Hexyl-CH_2), 1.57 (t, 3H, $J = 7.3$ Hz, Et), 1.62 (m, 2H, Hexyl-CH_2), 1.74 (t, 3H, $J = 7.3$ Hz, Et), 1.78 (t, 3H, $J = 7.3$ Hz, Et), 1.91 (t, 3H, $J = 7.3$ Hz, Et), 2.08 (m, 2H, rearranged-Et), 2.77 (q, 2H, $J = 7.3$ Hz, Et), 2.81 (m, 2H, rearranged-Et), 2.85 (q, 2H, $J = 7.3$ Hz, Et), 3.06 (q, 2H, $J = 7.3$ Hz, Et), 3.53 (t, 2H, Hexyl-CH_2), 3.59 (s, 6H, OMe), 3.79 (q, 2H, $J = 7.3$ Hz, Et), 3.82 (q, 2H, $J = 7.3$ Hz, Et), 3.97 (q, 2H, $J = 7.3$ Hz, Et), 5.26 (s, 2H, benzyl-CH_2), 5.64 (s, 1H, methylene-CH_2), 6.92 (s, 1H, methylene-CH_2), 6.94 (d, 2H, $J = 8.5$ Hz, Ar-H), 7.73 (t, 1H, $J = 8.5$ Hz, Ar-H), 7.96 (d, 2H, $J = 7.9$ Hz, Ar-H), 8.05 (s, 2H, Im-Ar-H), 8.33 (d, 2H, $J = 7.9$ Hz, Ar-H), 8.46 (d, 2H, $J = 7.9$ Hz, Ar-H), 8.48 (d, 2H, $J = 7.9$ Hz, Ar-H), 9.04 (d, 1H, $J = 4.3$ Hz, Por-β-H), 9.06 (d, 1H, $J = 4.3$ Hz, Por-β-H), 9.37 (s, 1H, Ch1-meso-H), 9.38 (d, 1H, $J = 4.3$ Hz, Por-β-H), 9.41 (d, 1H, $J = 4.3$ Hz, Por-β-H), 9.42 (d, 1H, $J = 4.3$ Hz, Por-β-H), 9.50 (d, 1H, $J = 4.3$ Hz, Por-β-H), 9.56 (d, 1H, $J = 4.3$ Hz, Por-β-H), 9.59 (d, 1H, $J = 4.3$ Hz, Por-β-H), 9.74 (s, 1H, Ch1-meso-H), 10.38 (s, 1H, Por-meso-H), 10.40 (s, 1H, Por-meso-H); HRMS (FAB) found, m/z 1520.6378; calcd for $C_{94}H_{90}O_6N_{10}Zn$, m/z 1520.6354 (M^+); IR (KBr) ν_{max} 1606 cm^{-1} (methylene-CH_2), 1720 cm^{-1} (CO).

ZC−ZP−I: mp >300 °C; ^{1}H-NMR ($CDCl_3$) 0.64 (t, 6H, rearranged-Et), 0.89 (t, 3H, hexyl-Me), 1.10 (t, 3H, $J = 7.3$ Hz, Et), 1.11 (t, 3H, $J = 7.3$ Hz, Et), 1.31 (m, 6H, hexyl-CH_2), 1.59 (t, 3H, $J = 7.3$ Hz, Et), 1.62 (m, 2H, hexyl-CH_2), 1.74 (t, 3H, $J = 7.3$ Hz, Et), 1.78 (t, 3H, $J = 7.3$ Hz, Et), 1.91 (t, 3H, $J = 7.3$ Hz, Et), 2.10 (m, 2H, rearranged-Et), 2.79 (q, 2H, $J = 7.3$ Hz, Et), 2.83 (m, 2H, rearranged-Et), 2.84 (q, 2H, $J = 7.3$ Hz, Et), 3.10 (q, 2H, $J = 7.3$ Hz, Et), 3.57 (t, 2H, hexyl-CH_2), 3.59 (s, 6H, OMe), 3.79 (q, 2H, $J = 7.3$ Hz, Et), 3.83 (q, 2H, $J = 7.3$ Hz, Et), 3.99 (q, 2H, $J = 7.3$ Hz, Et), 5.21 (s, 2H, benzyl-CH_2), 5.65 (s, 1H, methylene-CH_2), 6.93 (s, 1H, methylene-CH_2), 6.94 (d, 2H, $J = 8.5$ Hz, Ar-H), 7.73 (t, 1H, $J = 8.5$ Hz, Ar-H), 7.88 (d, 2H, $J = 7.8$ Hz, Ar-H), 8.04 (s, 2H, Im-Ar-H), 8.29 (d, 2H, $J = 7.8$ Hz, Ar-H), 8.43 (d, 2H, $J = 7.8$ Hz, Ar-H), 8.46 (d, 2H, $J = 7.8$ Hz, Ar-H), 9.10 (d, 1H, $J = 4.4$ Hz, Por-β-H), 9.10 (d, 1H, $J = 4.4$ Hz, Por-β-H), 9.38 (s, 1H, Ch1-meso-H), 9.42 (d, 1H, $J = 4.4$ Hz, Por-β-H), 9.43 (d, 1H, $J = 4.4$ Hz, Por-β-H), 9.44 (d, 1H, $J = 4.4$ Hz, Por-β-H), 9.57 (d, 1H, $J = 4.4$ Hz, Por-β-H), 9.58 (d, 1H, $J = 4.4$ Hz, Por-β-H), 9.61 (d, 1H, $J = 4.4$ Hz, Por-β-H), 9.74 (s, 1H, Ch1-meso-H), 10.37 (s, 1H, Por-meso-H), 10.37 (s, 1H, Por-meso-H); HRMS (FAB) found, m/z 1584.5426; calcd for $C_{94}H_{88}O_6N_{10}Zn_2$, m/z 1584.5461 (M^+); IR (KBr) ν_{max} 1616 cm^{-1} (methylene-CH_2), 1718 cm^{-1} (CO).

Synthesis of ZC−ZP−ZP−I: The dipyrrylmethane **10** (15 mg, 100 μmol), methylenechlorin **9** (48 mg, 60.8 μmol); and formyl-substituted porphyrin **13** (32 mg, 40 μmol) were dissolved in dry CH_2Cl_2 (50 mL). TFA (8 μL) was added to this solution, and the mixture was stirred for 16 h at room temperature under N_2 atmosphere in the dark. DDQ (34 mg) was added, and the resulting solution was stirred for an additional 6 h. The reaction was quenched with triethylamine (0.5 mL). After evaporation of the solvent, the residue was again dissolved in CH_2Cl_2 (30 mL). To this solution was added a saturated methanol solution of $Zn(OAc)_2$ (3 mL). The mixture was stirred at room temperature under N_2 atmosphere for 2 h. After usual workup, the products were separated by flash column chromatography on silica gel (CH_2Cl_2 eluent). Recrystallization from CH_2Cl_2/hexane gave free-base ZC−ZP−ZP−I (15 mg, 6 μmol).

Synthesis of ZC−HP and ZC−ZP. The methylenechlorin−porphyrin dyad HM−HP was prepared from **9**, *p*-tolualdehyde, and **10** in 61% yield in the same manner as described for HM−HP−I and was converted into ZC−HP and ZC−ZP in 15 and 30% yields, respectively.

HC−HP: mp >300 °C; ^{1}H-NMR ($CDCl_3$) −2.99 (br, 1H, Por-NH), −2.94 (br, 1H, Por-NH), −1.11 (s, 1H, Ch1-NH, the other peak of Ch1-NH was not detected), 0.60 (t, 6H, rearranged-Et), 1.14 (t, 3H, $J = 7.3$ Hz, Et), 1.18 (t, 3H, $J = 7.3$ Hz, Et), 1.65 (t, 3H, $J = 7.3$ Hz, Et), 1.80 (t, 3H, $J = 7.3$ Hz, Et), 1.86 (t, 3H, $J = 7.3$ Hz, Et), 1.96 (t, 3H, $J = 7.3$ Hz, Et), 2.14 (m, 2H, rearranged-Et), 2.75 (s, 3H, tolyl-Me), 2.81 (m, 2H, rearranged-Et), 2.86 (q, 2H, $J = 7.3$ Hz, Et), 3.02 (q, 2H, $J = 7.3$ Hz, Et), 3.28 (q, 2H, $J = 7.3$ Hz, Et), 3.57 (s, 6H,

OMe), 3.86 (q, 2H, *J* = 7.3 Hz, Et), 3.96 (q, 2H, *J* = 7.3 Hz, Et), 4.14 (q, 2H, *J* = 7.3 Hz, Et), 5.68 (s, 1H, methylene-CH_2), 6.93 (d, 2H, *J* = 8.6 Hz, Ar-H), 6.96 (s, 1H, methylene-CH_2), 7.64 (d, 2H, *J* = 7.9 Hz, Ar-H), 7.72 (t, 1H, *J* = 8.6 Hz, Ar-H), 8.20 (d, 2H, *J* = 7.9 Hz, Ar-H), 8.49 (d, 2H, *J* = 7.9 Hz, Ar-H), 8.51 (d, 2H, *J* = 7.9 Hz, Ar-H), 9.14 (d, 1H, *J* = 4.3 Hz, Por-β-H), 9.15 (d, 1H, *J* = 4.3 Hz, Por-β-H), 9.38 (d, 1H, *J* = 4.3 Hz, Por-β-H), 9.43 (d, 1H, *J* = 4.3 Hz, Por-β-H), 9.44 (d, 1H, *J* = 4.3 Hz, Por-β-H), 9.47 (d, 1H, *J* = 4.3 Hz, Por-β-H), 9.56 (d, 1H, *J* = 4.3 Hz, Por-β-H), 9.58 (d, 1H, *J* = 4.3 Hz, Por-β-H), 9.68 (s, 1H, Ch1-meso-H), 9.99 (s, 1H, Ch1-meso-H), 10.40 (s, 1H, Por-meso-H), 10.40 (s, 1H, Por-meso-H); HRMS (FAB) found, *m/z* 1159.6360; calcd for $C_{78}H_{78}O_2N_8$, *m/z* 1159.6327 (M^+ + H); IR (KBr) ν_{max} 1653 cm^{-1} (methylene-CH_2).

ZC−HP: mp >300 °C; ¹H-NMR (CDCl₃) −2.99 (br, 1H, Por-NH), −2.94 (br, 1H, Por-NH), 0.64 (t, 6H, rearranged-Et), 1.10 (t, 3H, *J* = 7.3 Hz, Et), 1.11 (t, 3H, *J* = 7.3 Hz, Et), 1.57 (t, 3H, *J* = 7.3 Hz, Et), 1.75 (t, 3H, *J* = 7.3 Hz, Et), 1.78 (t, 3H, *J* = 7.3 Hz, Et), 1.91 (t, 3H, *J* = 7.3 Hz, Et), 2.08 (m, 2H, rearranged-Et), 2.76 (s, 3H, tolyl-Me), 2.79 (m, 2H, rearranged-Et), 2.85 (q, 4H, *J* = 7.3 Hz, Et), 3.06 (q, 2H, *J* = 7.3 Hz, Et), 3.60 (s, 6H, OMe), 3.79 (q, 2H, *J* = 7.3 Hz, Et), 3.83 (q, 2H, *J* = 7.3 Hz, Et), 3.98 (q, 2H, *J* = 7.3 Hz, Et), 5.64 (s, 1H, methylene-CH_2), 6.92 (s, 1H, methylene-CH_2), 6.94 (d, 2H, *J* = 8.6 Hz, Ar-H), 7.65 (d, 2H, *J* = 7.9 Hz, Ar-H), 7.73 (t, 1H, *J* = 8.6 Hz, Ar-H), 8.20 (d, 2H, *J* = 7.9 Hz, Ar-H), 8.44 (d, 2H, *J* = 7.9 Hz, Ar-H), 8.47 (d, 2H, *J* = 7.9 Hz, Ar-H), 9.16 (d, 2H, *J* = 4.3 Hz, Por-β-H), 9.38 (s, 1H, Ch1-meso-H), 9.38 (d, 1H, *J* = 4.3 Hz, Por-β-H), 9.45 (d, 1H, *J* = 4.3 Hz, Por-β-H), 9.46 (d, 1H, *J* = 4.3 Hz, Por-β-H), 9.50 (d, 1H, *J* = 4.3 Hz, Por-β-H), 9.57 (d, 1H, *J* = 4.3 Hz, Por-β-H), 9.60 (d, 1H, *J* = 4.3 Hz, Por-β-H), 9.74 (s, 1H, Ch1-meso-H), 10.41 (s, 1H, Por-meso-H), 10.42 (s, 1H, Por-meso-H); HRMS (FAB) found, *m/z* 1220.5407; calcd for $C_{78}H_{76}O_2N_8Zn$, *m/z* 1220.5383 (M^+); IR (KBr) ν_{max} 1653 cm^{-1} (methylene-CH_2).

ZC−ZP: mp >300 °C; ¹H-NMR (CDCl₃) 0.65 (t, 6H, rearranged-Et), 1.10 (t, 3H, *J* = 7.8 Hz, Et), 1.11 (t, 3H, *J* = 7.8 Hz, Et), 1.59 (t, 3H, *J* = 7.8 Hz, Et), 1.75 (t, 3H, *J* = 7.8 Hz, Et), 1.79 (t, 3H, *J* = 7.8 Hz, Et), 1.92 (t, 3H, *J* = 7.8 Hz, Et), 2.11 (m, 2H, rearranged-Et), 2.77 (s, 3H, Tolyl-Me), 2.79 (m, 2H, rearranged-Et), 2.85 (q, 4H, *J* = 7.8 Hz, Et), 3.11 (q, 2H, *J* = 7.8 Hz, Et), 3.60 (s, 6H, OMe), 3.79 (q, 2H, *J* = 7.8 Hz, Et), 3.83 (q, 2H, *J* = 7.8 Hz, Et), 3.98 (q, 2H, *J* = 7.8 Hz, Et), 5.66 (s, 1H, methylene-CH_2), 6.93 (s, 1H, methylene-CH_2), 6.94 (d, 2H, *J* = 8.8 Hz, Ar-H), 7.64 (d, 2H, *J* = 7.8 Hz, Ar-H), 7.73 (t, 1H, *J* = 8.8 Hz, Ar-H), 8.20 (d, 2H, *J* = 7.8 Hz, Ar-H), 8.44 (d, 2H, *J* = 7.8 Hz, Ar-H), 8.46 (d, 2H, *J* = 7.8 Hz, Ar-H), 9.23 (d, 2H, *J* = 4.4 Hz, Por-β-H), 9.38 (s, 1H, Ch1-meso-H), 9.45 (d, 1H, *J* = 4.4 Hz, Por-β-H), 9.50 (d, 1H, *J* = 4.4 Hz, Por-β-H), 9.50 (d, 1H, *J* = 4.4 Hz, Por-β-H), 9.59 (d, 1H, *J* = 4.4 Hz, Por-β-H), 9.62 (d, 1H, *J* = 4.4 Hz, Por-β-H), 9.65 (d, 1H, *J* = 4.4 Hz, Por-β-H), 9.74 (s, 1H, Ch1-meso-H), 10.42 (s, 1H, Por-meso-H), 10.44 (s, 1H, Por-meso-H); HRMS (FAB) found, *m/z* 1286.4518; calcd for $C_{78}H_{74}O_2N_8Zn_2$, *m/z* 1286.4499 (M^+); IR (KBr) ν_{max} 1653 cm^{-1} (methylene-CH_2).

Synthesis of ZP−I, HP−I, ZP, and HP. The dipyrrylmethane **10** (105 mg, 0.72 mmol), *p*-toluadehyde (72 mg, 0.60 mmol), and **11** (50 mg, 0.12 mmol) were dissolved in CH_2Cl_2 (50 mL). TFA (55 μL) (82 mg, 0.72 mmol) was added to this solution, and the mixture was stirred for 6 h at room temperature under N_2 atmosphere in the dark. DDQ (212 mg, 0.94 mmol) was added, and the resulting solution was stirred for an additional 2 h. The reaction mixture was treated with 3 N HCl and aqueous Na_2CO_3 and dried over anhydrous Na_2SO_4. After evaporation of the solvent, the residue was separated by flash column chromatography on silica gel (CHCl₃ eluent). The first fraction was collected, and the organic solvent was evaporated. Recrystallization from CH_2Cl_2/MeOH gave HP as violet crystals (50.0 mg, 0.10 mmol) in 28% yield based on the amount of **10** used. Similarly, HP−I (28.0 mg, 0.04 mmol) was obtained from the second fraction in 10% yield. Porphyrins ZP and ZP−I were prepared from HP and HP−I by the usual Zn insertion (Zn(OAc)₂, CH_2Cl_2/MeOH, reflux) in 50 and 79% yields, respectively.

ZP−I: mp >300 °C; ¹H-NMR (CDCl₃) 0.90 (t, 3H, hexyl-Me), 1.35 (m, 6H, hexyl-CH_2), 1.73 (m, 2H, hexyl-CH_2), 2.75 (s, 3H, tolyl-Me), 3.76 (t, 2H, hexyl-CH_2), 5.30 (s, 2H, benzyl-CH_2), 7.60 (d, 2H, *J* = 8.3 Hz, Ar-H), 7.86 (d, 2H, *J* = 8.3 Hz, Ar-H), 8.15 (d, 2H, *J* = 8.3 Hz, Ar-H), 8.25 (d, 2H, *J* = 8.3 Hz, Ar-H), 8.39 (s, 2H, Im-Ar-H), 9.10 (d, 2H, *J* = 4.4 Hz, Por-β-H), 9.18 (d, 2H, *J* = 4.4 Hz, Por-β-H), 9.43 (d, 2H, *J* = 4.4 Hz, Por-β-H), 9.44 (d, 2H, *J* = 4.4 Hz, Por-β-H), 10.32 (s, 2H, meso-H); HRMS (FAB) found, *m/z* 850.2238; calcd for $C_{50}H_{38}O_4N_6Zn$, *m/z* 850.2246 (M^+).

HP−I: mp >300 °C; ¹H-NMR (CDCl₃) −3.19 (br, 2H, NH), 0.88 (t, 3H, hexyl-Me), 1.31 (m, 6H, hexyl-CH_2), 1.65 (m, 2H, hexyl-CH_2), 2.74 (s, 3H, tolyl-Me), 3.60 (t, 2H, hexyl-CH_2), 5.25 (s, 2H, benzyl-CH_2), 7.62 (d, 2H, *J* = 7.0 Hz, Ar-H), 7.91 (d, 2H, *J* = 8.0 Hz, Ar-H), 8.16 (s, 2H, Im-Ar-H), 8.17 (d, 2H, *J* = 7.0 Hz, Ar-H), 8.28 (d, 2H, *J* = 8.0 Hz, Ar-H), 9.01 (d, 2H, *J* = 4.6 Hz, Por-β-H), 9.11 (d, 2H, *J* = 4.6 Hz, Por-β-H), 9.36 (d, 2H, *J* = 4.6 Hz, Por-β-H), 9.38 (d, 2H, *J* = 4.6 Hz, Por-β-H), 10.28 (s, 2H, meso-H); HRMS (FAB) found, *m/z* 789.3171; calcd for $C_{50}H_{40}O_4N_6$, *m/z* 789.3190 (M^+ + H).

ZP: mp >300 °C; ¹H-NMR (CDCl₃) 2.75 (s, 6H, tolyl-Me), 7.60 (d, 4H, *J* = 7.6 Hz, Ar-H), 8.14 (d, 4H, *J* = 7.6 Hz, Ar-H), 9.16 (d, 4H, *J* = 4.4 Hz, Por-β-H), 9.41 (d, 4H, *J* = 4.4 Hz, Por-β-H), 10.28 (s, 2H, meso-H); HRMS (FAB) found, *m/z* 552.1366; calcd for $C_{34}H_{24}N_4Zn$, *m/z* 552.1292 (M^+).

HP: mp >300 °C; ¹H-NMR (CDCl₃) −3.09 (br, 2H, NH), 2.74 (s, 6H, Tolyl-Me), 7.62 (d, 4H, *J* = 7.7 Hz, Ar-H), 8.16 (d, 4H, *J* = 7.7 Hz, Ar-H), 9.11 (d, 4H, *J* = 4.9 Hz, Por-β-H), 9.39 (d, 4H, *J* = 4.9 Hz, Por-β-H), 10.30 (s, 2H, meso-H); HRMS (FAB) found, *m/z* 490.2131; calcd for $C_{34}H_{26}N_4$, *m/z* 490.2157 (M^+).

Synthesis of ZC. The reference methylenechlorin (HC) was prepared from the corresponding oxochlorin precursors in 62 and 84% yields in the essentially same manner as described for **7** and **8**, respectively, and was converted into HC in quantitative yield.

HC: mp >300 °C; ¹H-NMR (CDCl₃) 0.37 (t, 6H, rearranged-Et), 1.04 (t, 3H, *J* = 7.3 Hz, Et), 1.05 (t, 3H, *J* = 7.3 Hz, Et), 1.06 (t, 3H, *J* = 7.3 Hz, Et), 1.63 (m, 2H, rearranged-Et), 1.67 (t, 3H, *J* = 7.3 Hz, Et), 1.71 (t, 3H, *J* = 7.3 Hz, Et), 1.73 (t, 3H, *J* = 7.3 Hz, Et), 2.20 (m, 2H, rearranged-Et), 2.26 (q, 2H, *J* = 7.3 Hz, Et), 2.74 (q, 2H, *J* = 7.3 Hz, Et), 2.80 (q, 2H, *J* = 7.3 Hz, Et), 3.55 (s, 6H, OMe), 3.72 (q, 2H, *J* = 7.3 Hz, Et), 3.76 (q, 4H, *J* = 7.3 Hz, Et), 5.40 (s, 1H, methylene-CH_2), 6.76 (s, 1H, methylene-CH_2), 6.90 (d, 2H, *J* = 8.5 Hz, Ar-H), 7.50 (dd, 2H, *J* = 7.3, 7.3 Hz, Ar-H), 7.65 (t, 1H, *J* = 7.3 Hz, Ar-H), 7.70 (t, 1H, *J* = 8.5 Hz, Ar-H), 7.99 (d, 2H, *J* = 7.3 Hz, Ar-H), 9.25 (s, 1H, meso-H), 9.60 (s, 1H, meso-H); HRMS (FAB) found, *m/z* 822.3808; calcd for $C_{51}H_{58}O_2N_4Zn$, *m/z* 822.3851 (M^+); IR (KBr) ν_{max} 1624 cm^{-1} (methylene-CH_2).

ZC: mp 285−286 °C; ¹H-NMR (CDCl₃) −1.32 (s, 1H, NH), −0.23 (br, 1H, NH), 0.35 (t, 6H, rearranged-Et), 1.09 (t, 3H, *J* = 7.3 Hz, Et), 1.12 (t, 3H, *J* = 7.3 Hz, Et), 1.13 (t, 3H, *J* = 7.3 Hz, Et), 1.72 (t, 3H, *J* = 7.3 Hz, Et), 1.72 (m, 2H, rearranged-Et), 1.78 (t, 3H, *J* = 7.3 Hz, Et), 1.78 (t, 3H, *J* = 7.3 Hz, Et), 2.22 (m, 2H, rearranged-Et), 2.51 (q, 2H, *J* = 7.3 Hz, Et), 2.81 (q, 2H, *J* = 7.3 Hz, Et), 2.97 (q, 2H, *J* = 7.3 Hz, Et), 3.54 (s, 6H, OMe), 3.79 (q, 2H, *J* = 7.3 Hz, Et), 3.89 (q, 2H, *J* = 7.3 Hz, Et), 3.92 (q, 2H, *J* = 7.3 Hz, Et), 5.45 (s, 1H, methylene-CH_2), 6.80 (s, 1H, methylene-CH_2), 6.91 (d, 2H, *J* = 8.5 Hz, Ar-H), 7.56 (dd, 2H, *J* = 7.3, 7.5 Hz, Ar-H), 7.70 (t, 1H, *J* = 7.5 Hz, Ar-H), 7.70 (t, 1H, *J* = 8.5 Hz, Ar-H), 8.03 (d, 2H, *J* = 7.3 Hz, Ar-H), 9.55 (s, 1H, meso-H), 9.85 (s, 1H, meso-H); HRMS (FAB) found, *m/z* 761.4792; calcd for $C_{51}H_{60}O_2N_4$, *m/z* 761.4795 (M^+ + H); IR (KBr) ν_{max} 1633 cm^{-1} (methylene-CH_2).